1,3,4-oxadiazole-functionalized *α*-aminophosphonates as ligand for the ruthenium-catalyzed reduction of ketones

Shaima Hkiri, Christophe Gourlaouen, Soufiane Touil, Ali Samarat, David Sémeril

Contents

Computational details

1. Methods

All calculations were performed with the Gaussian 09 program,[1] using the functional ωB97XD. Dispersion corrections were included.[2] All atoms were described using the 6-31+G** basis set except the ruthenium atom described by the SDD basis set and associated pseudopotential. The structure was fully optimised and the wavefunction saved. The free enthalpy was extracted from the frequency calculation performed on this geometry. The weak interactions were studied through the NCI analysis[3] of Gaussian wavefunction. All calculations were performed in the gas phase.

[1] M. J. Frisch, G. W. Trucks, H. B. Schlegel, G. E. Scuseria, M. A. Robb, J. R. Cheeseman, G. Scalmani, V. Barone, B. Mennucci, G. A. Petersson, H. Nakatsuji, M. Caricato, X. Li, H. P. Hratchian, A. F. Izmaylov, J. Bloino, G. Zheng, J. L. Sonnenberg, M. Hada, M. Ehara, K. Toyota, R. Fukuda, J. Hasegawa, M. Ishida, T. Nakajima, Y. Honda, O. Kitao, H. Nakai, T. Vreven, J. A. Montgomery Jr., J. E. Peralta, F. Ogliaro, M. Bearpark, J. J. Heyd, E. Brothers, K. N. Kudin, V. N. Staroverov, R. Kobayashi, J. Normand, K. Raghavachari, A. Rendell, J. C. Burant, S. S. Iyengar, J. Tomasi, M. Cossi, N. Rega, J. M. Millam, M. Klene, J. E. Knox, J. B. Cross, V. Bakken, C. Adamo, J. Jaramillo, R. Gomperts, R. E. Stratmann, O. Yazyev, A. J. Austin, R. Cammi, C. Pomelli, J. W. Ochterski, R. L. Martin, K. Morokuma, V. G. Zakrzewski, G. A. Voth, P. Salvador, J. J. Dannenberg, S. Dapprich, A. D. Daniels, O. Farkas, J. B. Foresman, J. V. Ortiz, J. Cioslowski, D. J. Fox, *Gaussian 09, Revision D.01, Gaussian Inc*., Wallingford CT, **2009**.

[2] S. Grimme, J. Antony, S. Ehrlich, H. Krieg, *J. Chem. Phys*., **2010**, *132*, 154104.

[3] J. Contreras-Garcia, E. R. Johnson, S. Keinan, R. Chaudret, J.-P. Piquemal, D. N. Beratan, W. T. Yang, *J. Chem. Theory Comput*., **2011**, *7*, 625-632.

2. Ligands

To determine the influence of different chemical functionalities on the properties of the ligand **3a**, several fragments were studied (**L1-L5**; Figure S1). To understand the role played by the conjugation between the phenyl and the oxadiazole rings and by the hydrogen bond, rotations around dihedral angles N2-C2-C-C (R1 in **3a**) and N1-C1-N-H (R2 in **3a**) were performed.

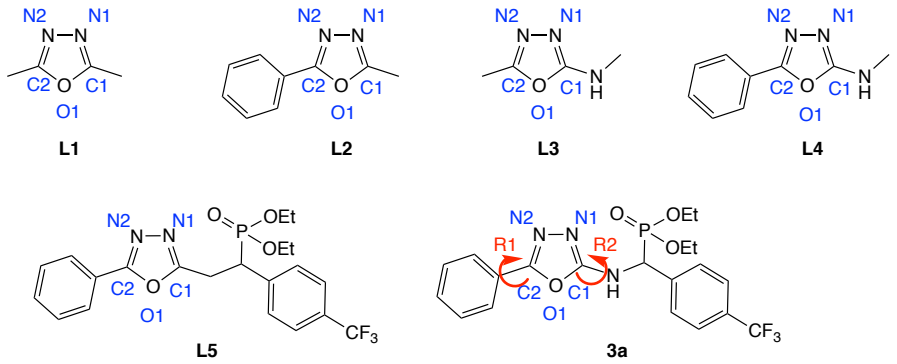

Figure S1: Studied ligands.

To understand the influence of the substituents of the oxadiazole ring on its electronic structure, a study of the natural bond orbital charges was carried out (Table S1). Starting from the symmetrical dimethyl substituted oxadiazole (**L1**), introduction of a phenyl on C2 (**L2**) has almost no influence despite the conjugation between the two aromatic cycles as proved by the value of the dihedral angle N2-C2-C-C, which oscillates between 0 and 5° in all the structures, the two cycles are coplanar (a structure for which the dihedral angle N2-C2-C-C is forced at 90° is 6.8 kcal.mol^{-1} less stable). The presence of the amine moiety polarises the oxadiazole ring (**L3**, **L4** and **3a)**. If N2 is only slightly affected, there are strong effects on N1 (more electron rich) and on C1 (less electron rich). The rest of the ligand has no effect as shown when comparing **3a** and **L4**.

Table S1: Natural bond orbital charge analysis.

	O	C1	N1	N2	C2
L1	-0.50	0.51	-0.33	-0.33	O.51
L2	-0.49	0.52	-0.32	-0.32	0.52
L3	-0.52	0.70	-0.40	-0.31	0.49
L4	-0.51	0.71	-0.40	-0.30	0.50
L5	-0.49	0.53	-0.31	-0.31	0.52
3a	-0.51	0.71	-0.38	-0.30	0.50

3. Ruthenium complexes

Several ruthenium complexes were optimised in which ligands **3a** and **L5** are coordinated to the metal *via* their N1 or N2 atoms (Figure S2).

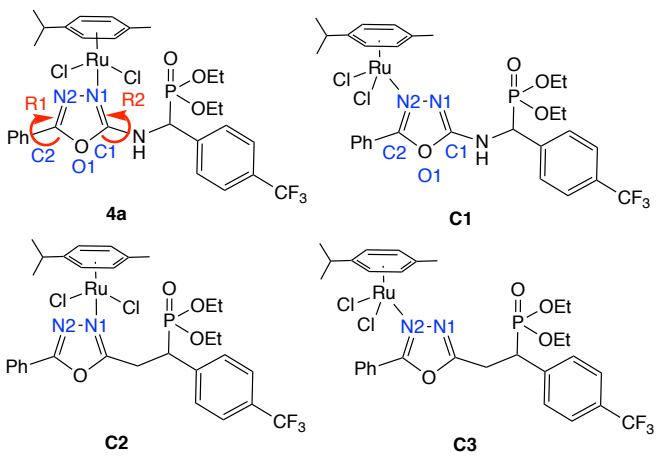

Figure S2: Studied ruthenium complexes.

In complex **4a**, the dihedral angle N2-C2-C-C is larger (10.2°) indicating a slight distortion of the ligand structure with a Ru-N1 length of 2.132 Å. The calculation found the presence of a hydrogen bond between the NH and one chloride atom and a conjugation between the amine and the oxadiazole ring with a C1-NH distance of 1.327 Å and a dihedral angle N1-C1-N-H of 173.1°, value close to those of an imine (dihedral angle of 180°). Replacement of the amine with a CH_2 (**C2**) slightly increases the Ru-N1 bond (2.153 Å) with a dihedral angle N2-C2-C-C of 14.3°. Coordination by the nitrogen N2 (**C1**) lengthens the Ru-N bond (Ru-N2 length is 2.172 Å) and requires a rotation of the phenyl ring (dihedral angle N2-C2-C-C = 46°). In the amine free complex (**C3**) the Ru-N2 length is not modified (2.179 Å) and the dihedral angle N2-C2-C-C is slightly reduced (39.7°). The rotation around the dihedral angle N1-C1-N-H has a profound influence on the structure. In **4a**, when the dihedral angle N1-C1-N-H is stabilised at -8.4°, the distance Ru-N1 length is longest (2.232 Å) and the dihedral angle N2-C2-C-C remains at an optimal value of 8.2°.

Whatever the ligand employed, with (**3a**) or without amine (**L5**), coordination *via* N1 atom is always favoured. Ruthenium complexes **4a** or **C2** are more stable than **C1** or **C3** (15.8 and 7.8 $kcal.mol^{-1}$, respectively; Table S2). Breaking the NH•••Cl hydrogen bond (**4a** with a dihedral angle N1-C1-N-H of -8.4°) destabilises the complex (12.9 $kcal.mol^{-1}$). This attempt to quantify the contribution of the NH•••Cl hydrogen bond fails. Unfortunately, it seems that steric constraints between to the phosphate group and to the phenyl-CF_3 moiety come into play and partly explains the extension of the Ru-N1 bond. There is also a depolarization of oxadiazole ring, the charge carried by N1 (-0.32 electrons) is similar to that carried by N2 (-0.30 electrons) due to the weaker conjugation between the NH and the oxadiazole ring (dihedral angle C-N-H-C of 152.3°).

Coordination *via* the less basic nitrogen atom N2 (**C1**) leads to a rupture of the NH•••Cl hydrogen bond, a longer Ru-N2 bond, a lower conjugation between the phenyl and the oxadiazole rings (dihedral angle N2-C2-C-C = 46°) and finally a destabilisation of the complex (15.8 $kcal.mol^{-1}$). From Table S2, we can conclude that three parameters promote coordination of the nitrogen atom N1 to the ruthenium:

- the presence of a NH•••Cl hydrogen bond;
- the higher basicity of N1;
- the steric constraints highlighted by evolution of the dihedral angle N2-C2-C-C, which breaks the conjugation between phenyl and oxadiazole rings.

Table S2: Relative energy of the structures (ΔG kcal.mol^{-1}) compared to **4a** and **C2**.

Complex	ΔG (kcal.mol^{-1})
4a (dihedral angle N1-C1-N-H = 173.1°)	0
4a (dihedral angle N1-C1-N-H = -8.4°)	12.9
C1	15.8
C2	0
C3	7.8

(*E*)-1-(4-trifluoromethylphenyl)-*N*-(5-phenyl-1,3,4-oxadiazol-2-yl)methanimine (2a)

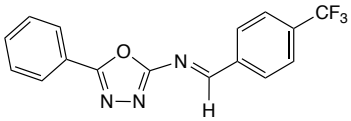

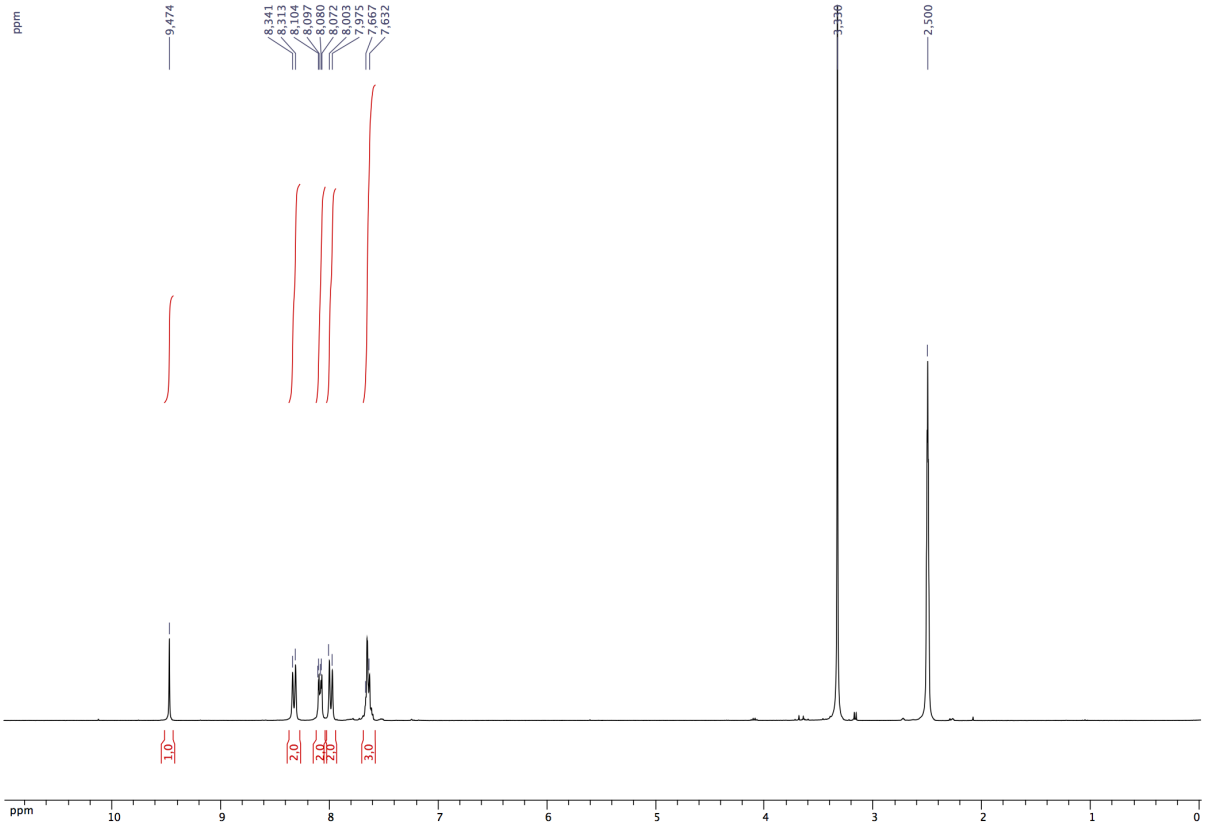

^{1}H NMR spectrum (DMSO-d_6)

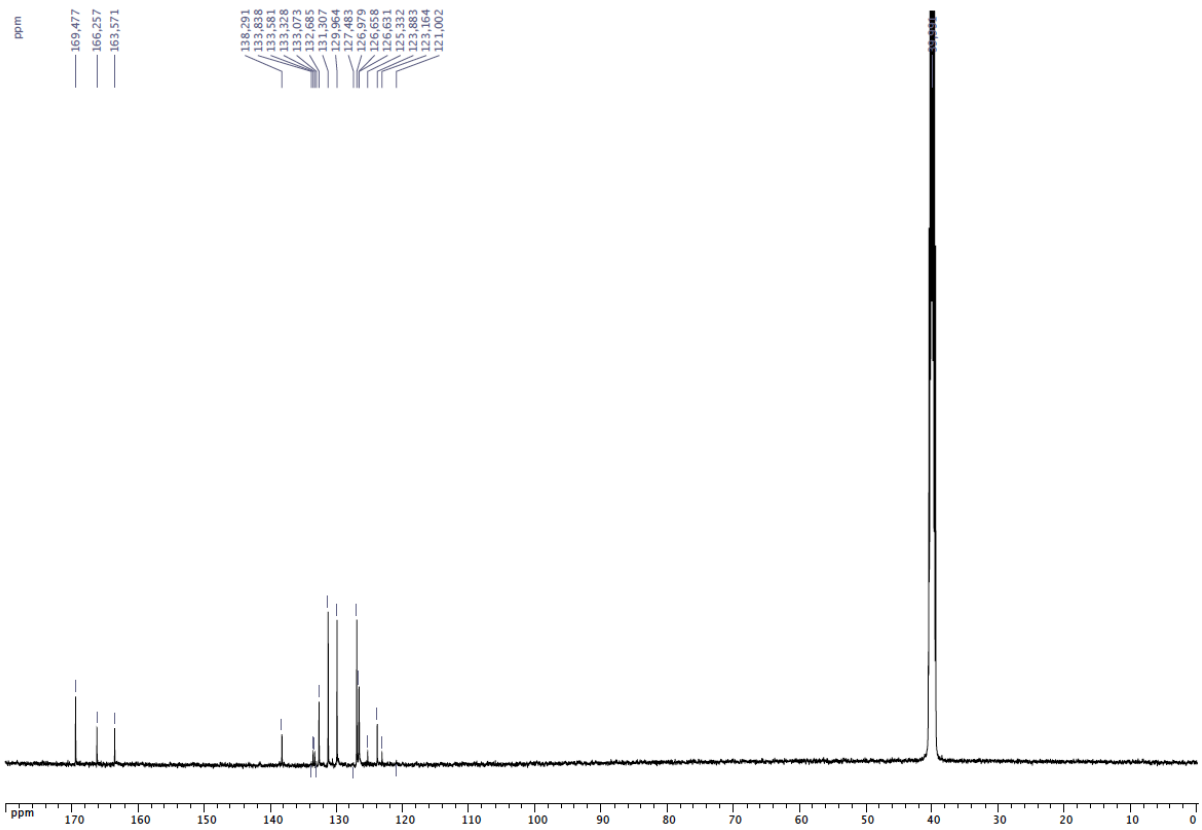

$^{13}C\{^{1}H\}$ NMR spectrum (DMSO-d_6)

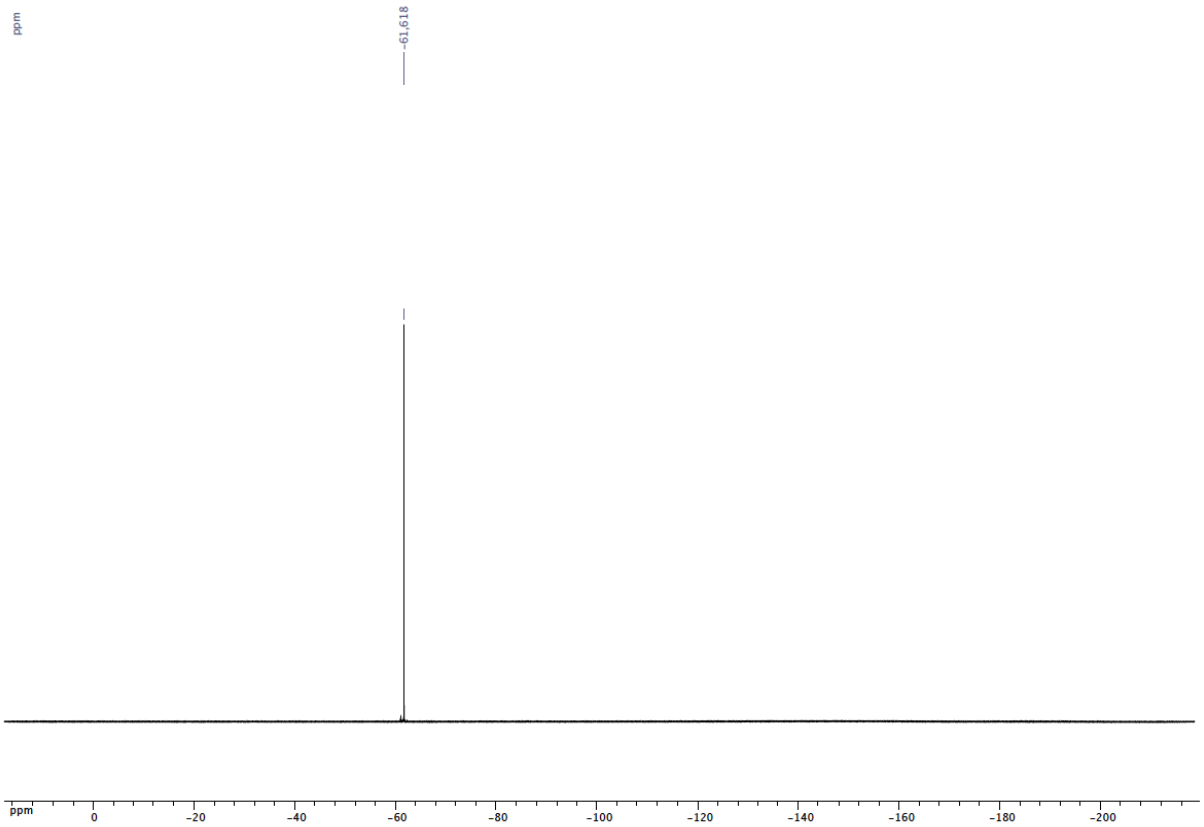

$^{19}F\{^{1}H\}$ NMR spectrum (DMSO-d_6)

(*E*)-1-(2-methoxyphenyl)-*N*-(5-phenyl-1,3,4-oxadiazol-2-yl)methanimine (2b)

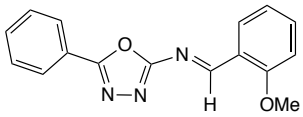

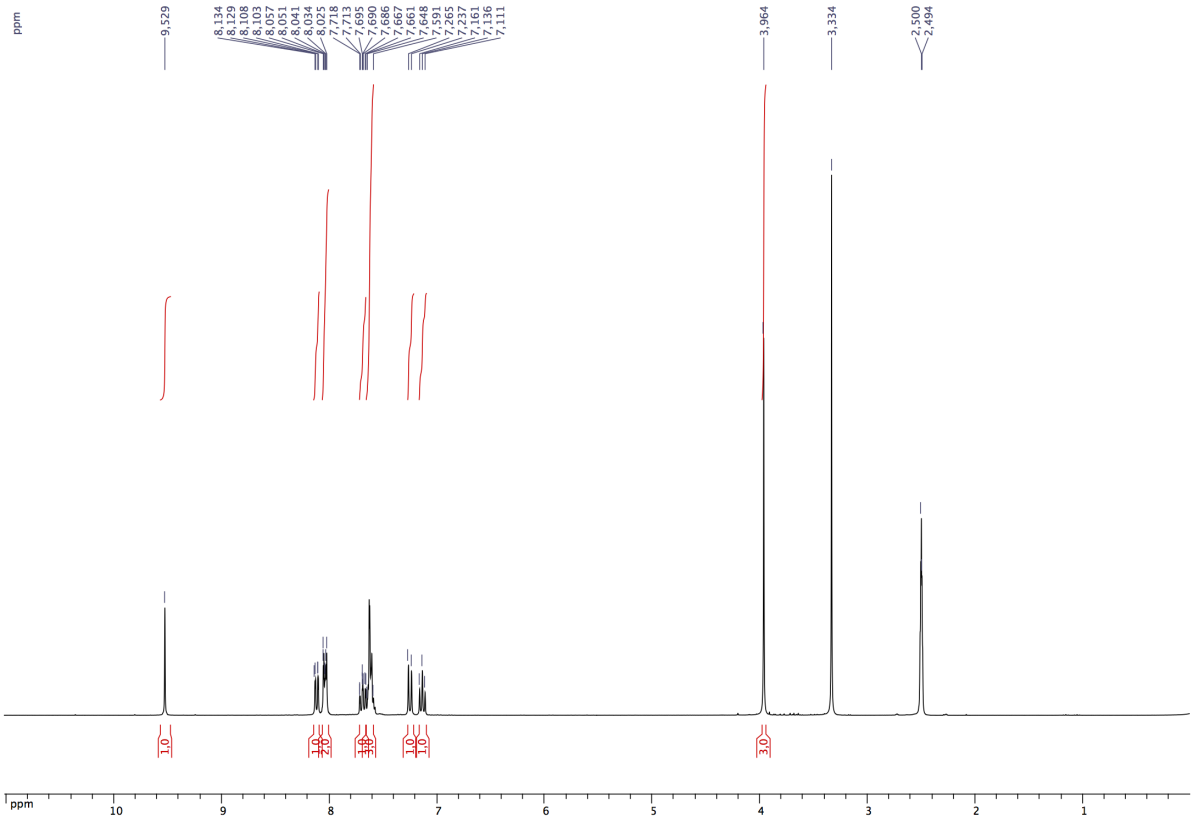

^{1}H NMR spectrum (DMSO-d_6)

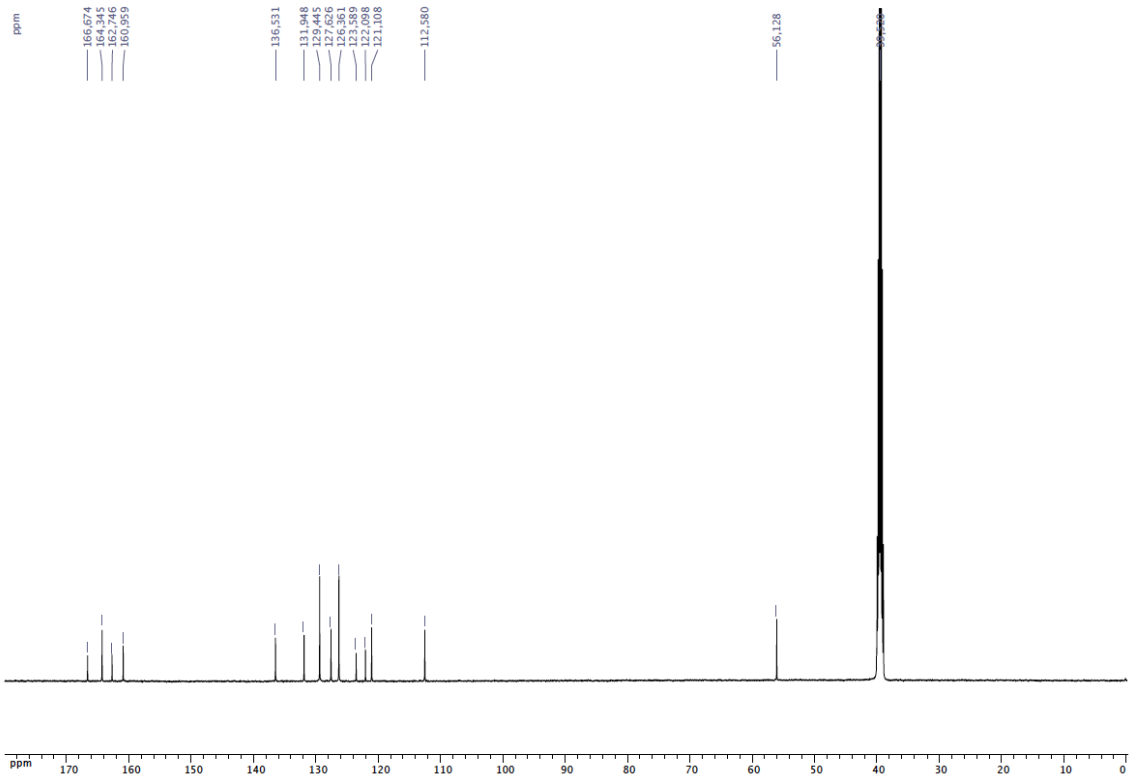

$^{13}C\{^{1}H\}$ NMR spectrum (DMSO-d_6)

(*E*)-1-(4-Nitrophenyl)-*N*-(5-phenyl-1,3,4-oxadiazol-2-yl)methanimine (2c)

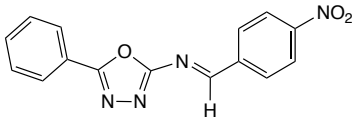

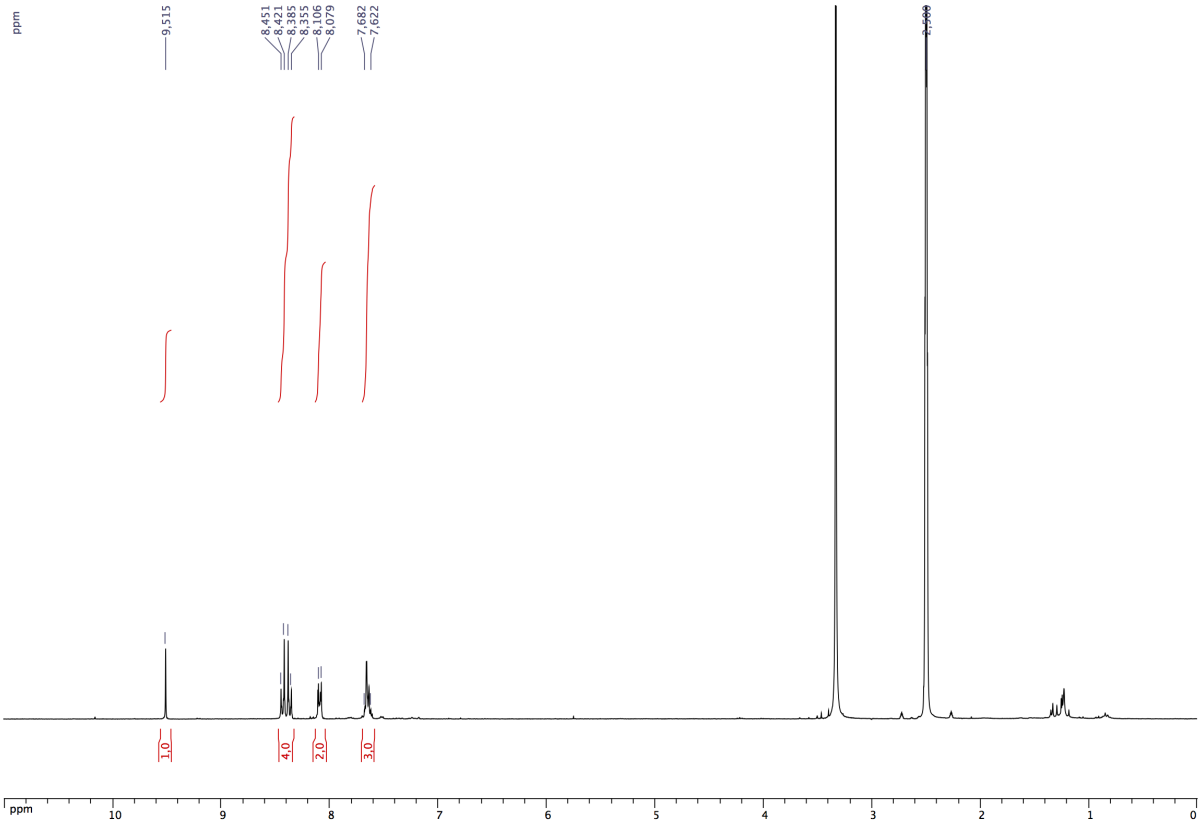

^{1}H NMR spectrum (DMSO-d_6)

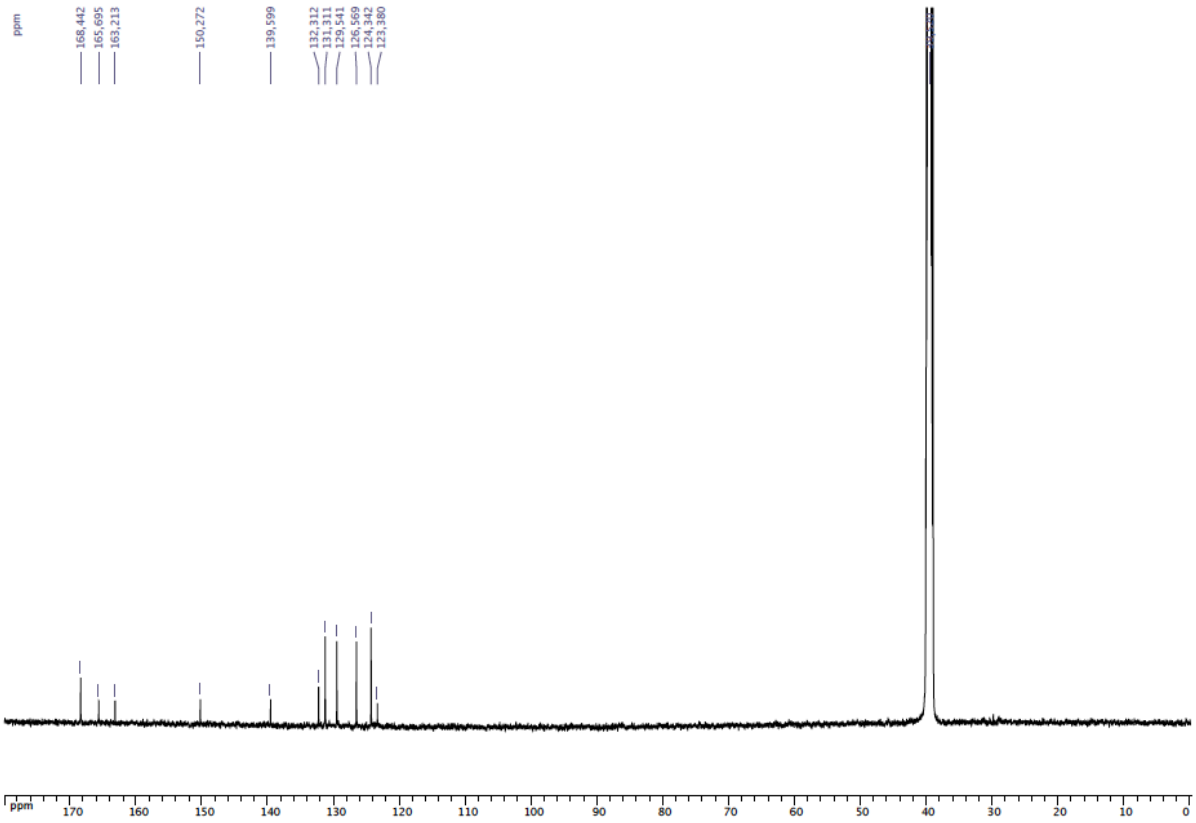

$^{13}C\{^{1}H\}$ NMR spectrum (DMSO-d_6)

l-1,3,4-axodiazol-2-ylamino)(4-trifluoromethylphenyl) methyl]phosphonate (3a)

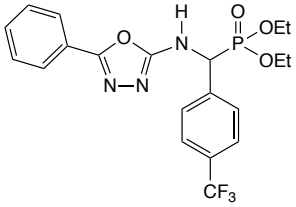

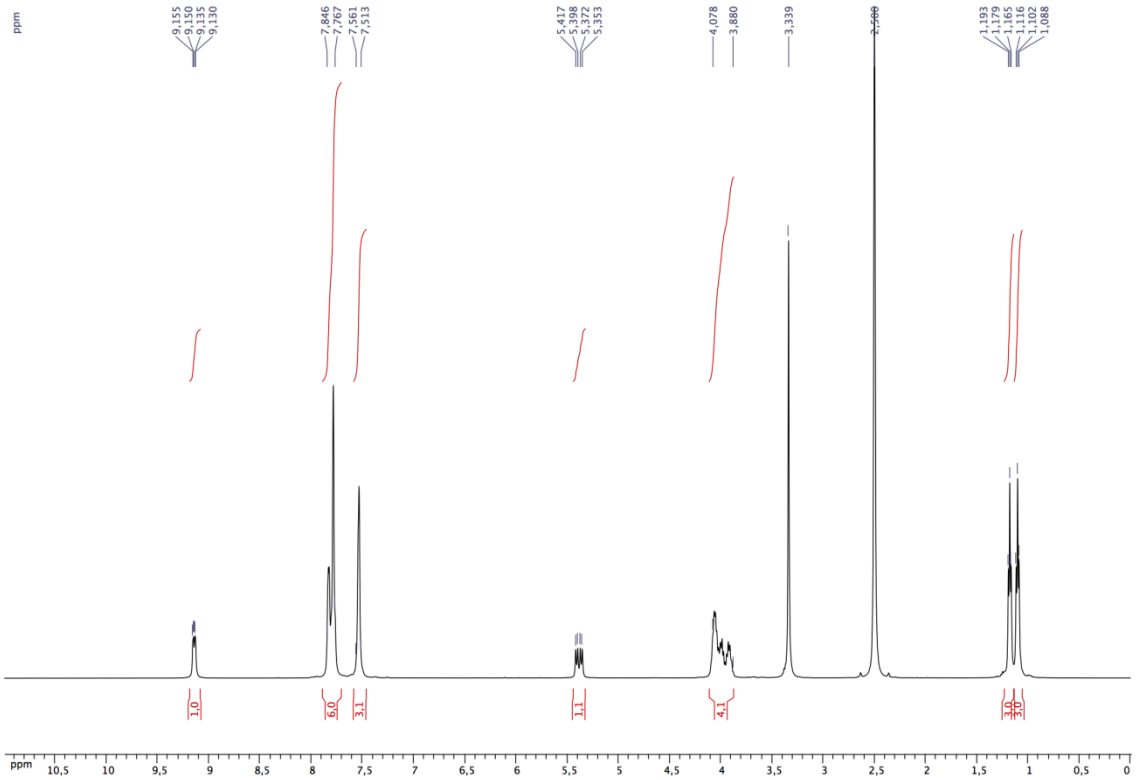

^{1}H NMR spectrum (DMSO-d_6)

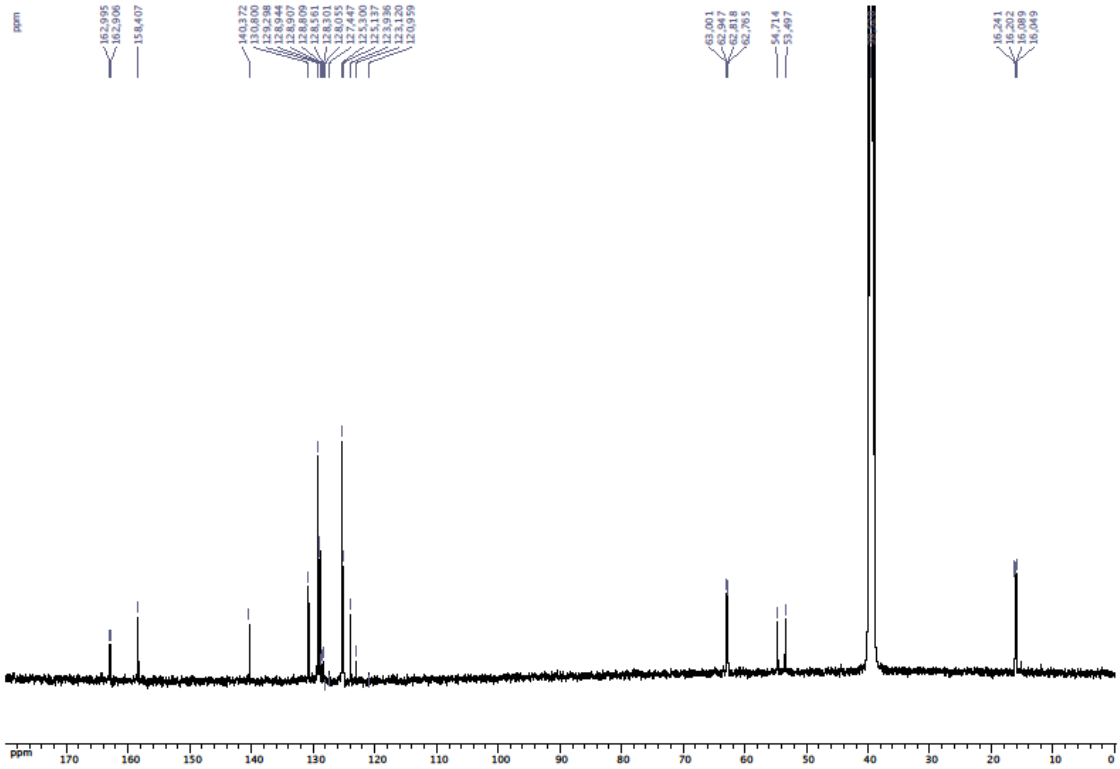

$^{13}C\{^{1}H\}$ NMR spectrum (DMSO-d_6)

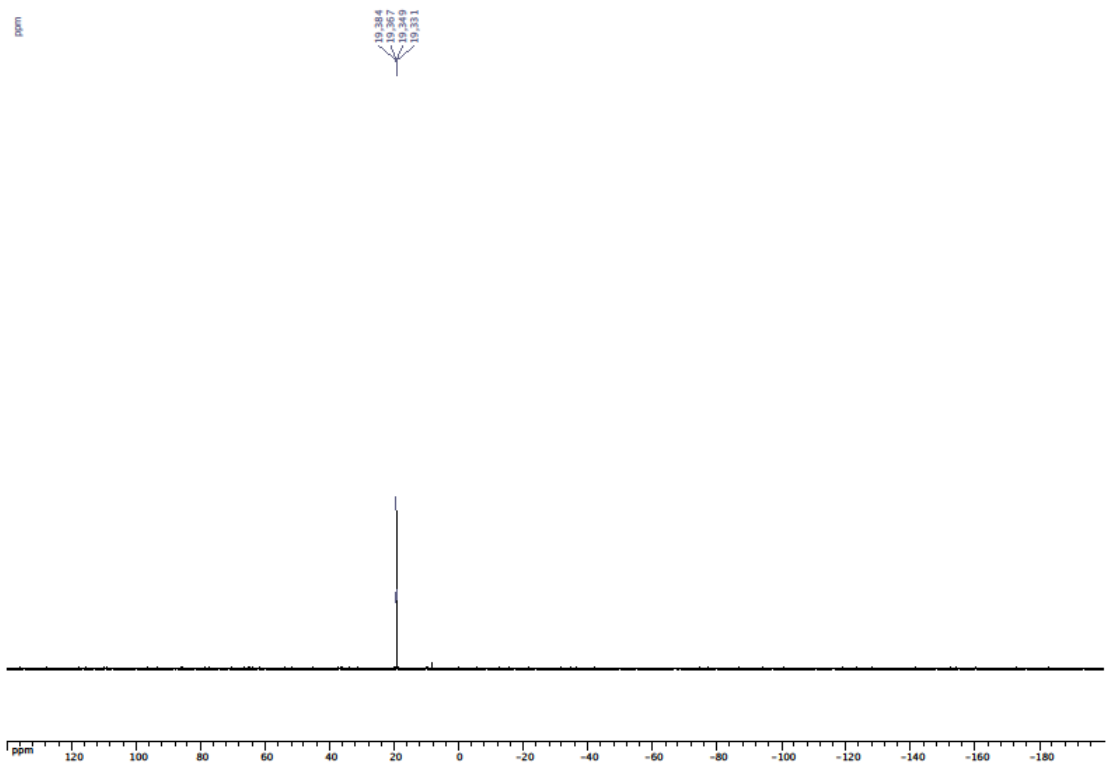

$^{31}P\{^{1}H\}$ NMR spectrum (DMSO-d_6)

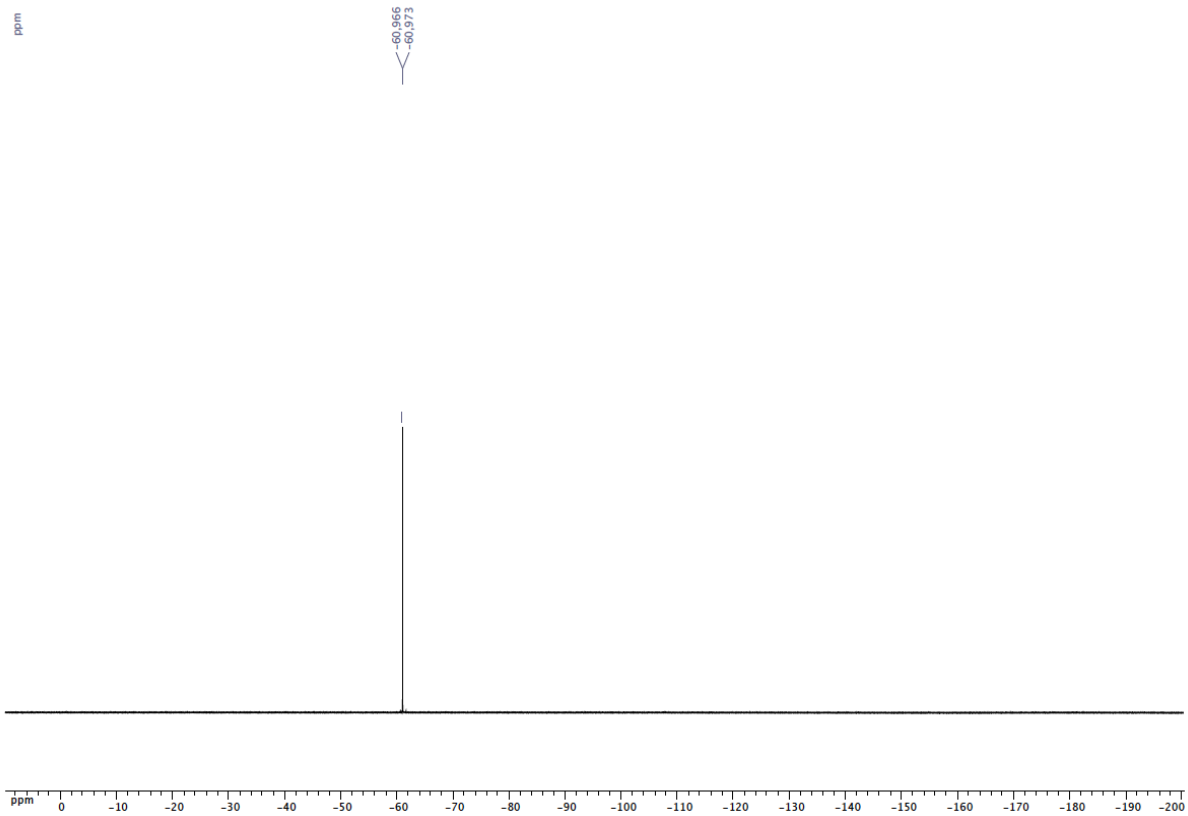

$^{19}F\{^{1}H\}$ NMR spectrum (DMSO-d_6)

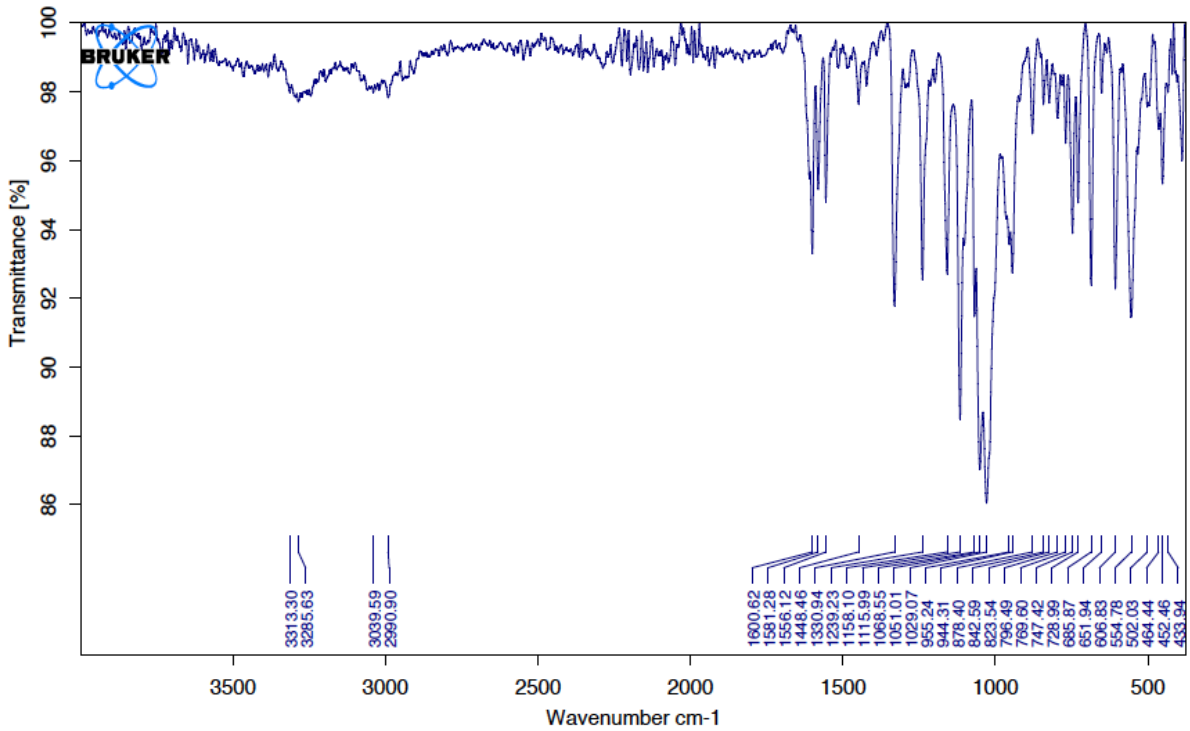

FT-IR spectrum

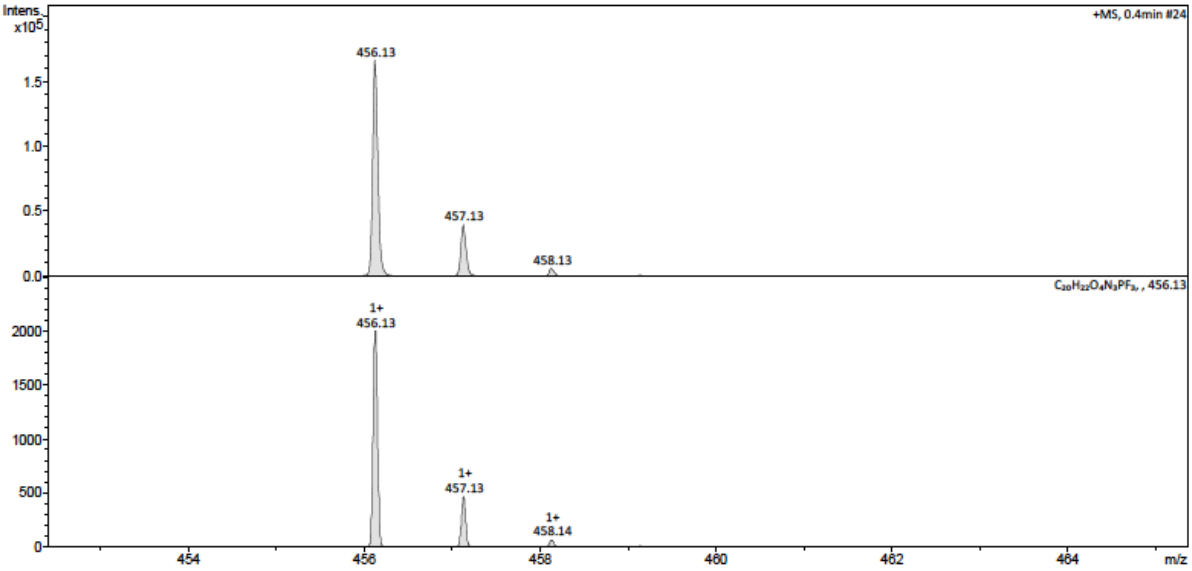

Mass spectrum (ESI-TOF)
exp. spectrum (top); calc. spectrum (bottom) for $C_{20}H_{21}O_4N_3PF_3$ + H

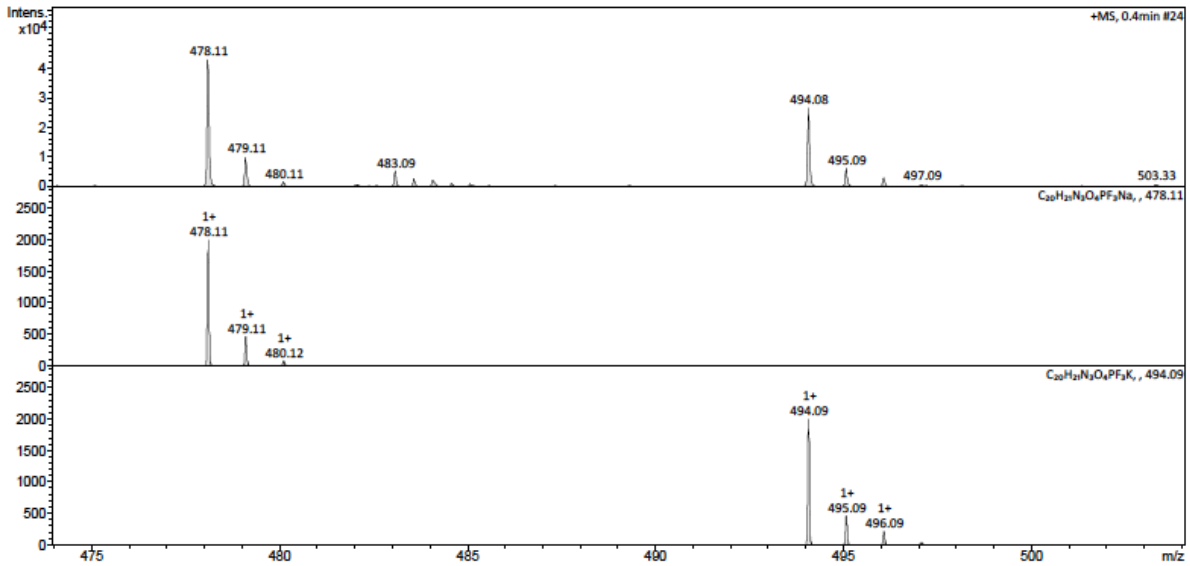

Mass spectrum (ESI-TOF)
exp. spectrum (top); calc. spectrum (middle) for $C_{20}H_{21}O_4N_3PF_3$ + Na;
calc. spectrum (bottom) for $C_{20}H_{21}O_4N_3PF_3$ + K

Diethyl[(5-phenyl-1,3,4-axodiazol-2-ylamino)(2-methoxyphenyl) methyl]phosphonate (3b)

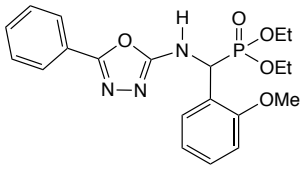

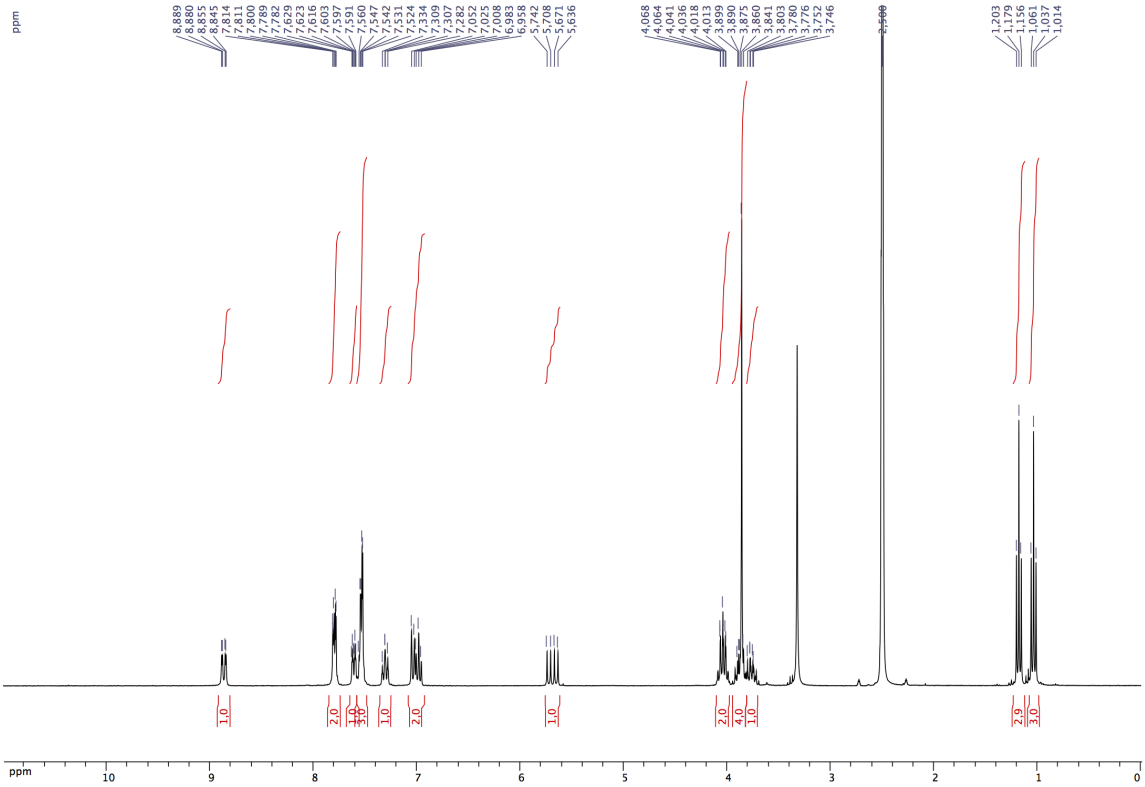

^{1}H NMR spectrum (DMSO-d_6)

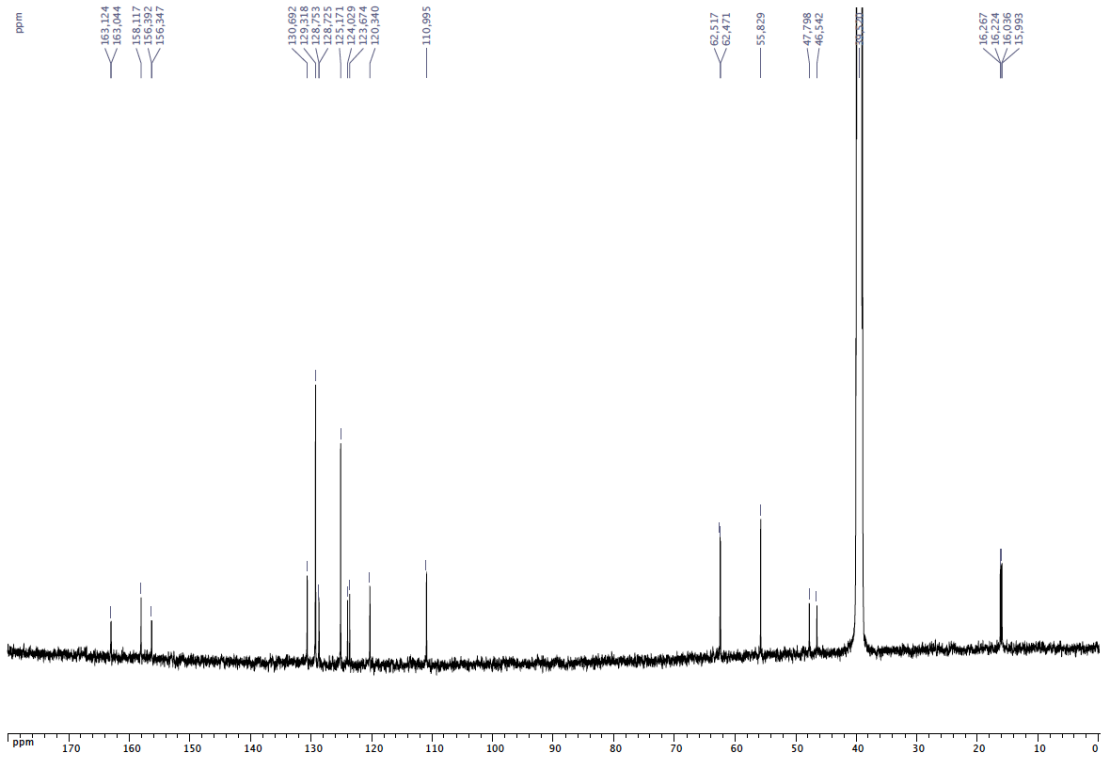

$^{13}C\{^{1}H\}$ NMR spectrum (DMSO-d_6)

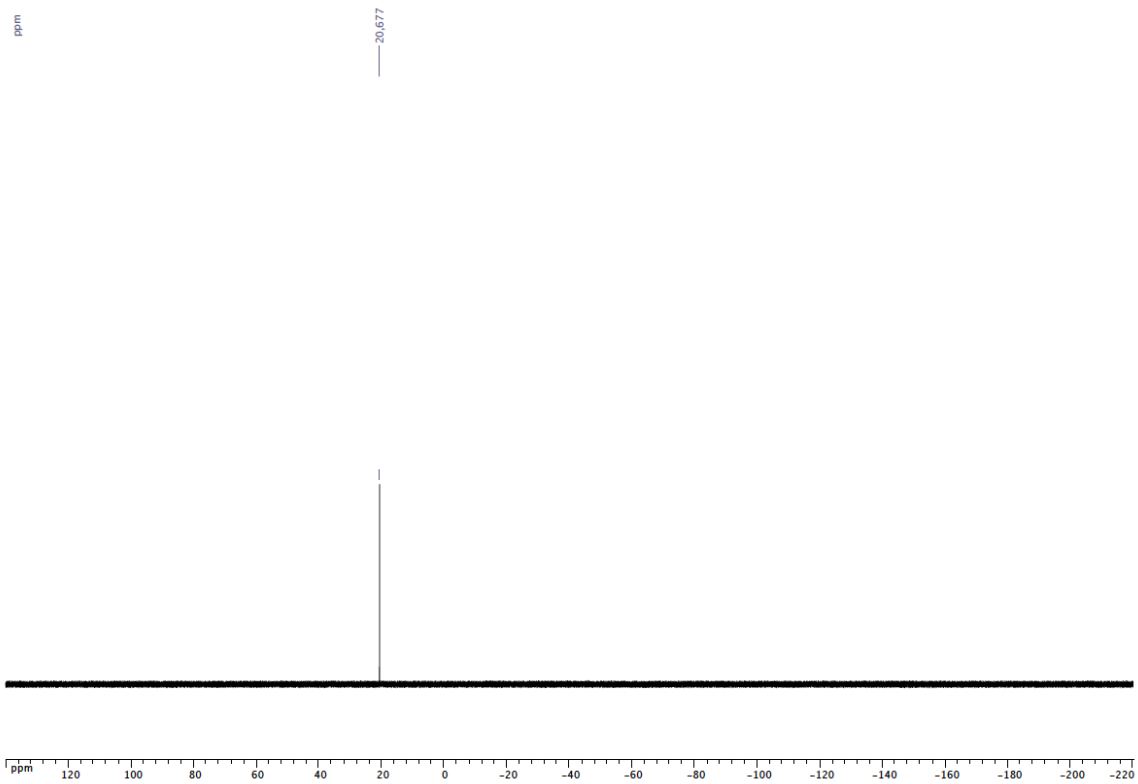

$^{31}P\{^{1}H\}$ NMR spectrum (DMSO-d_6)

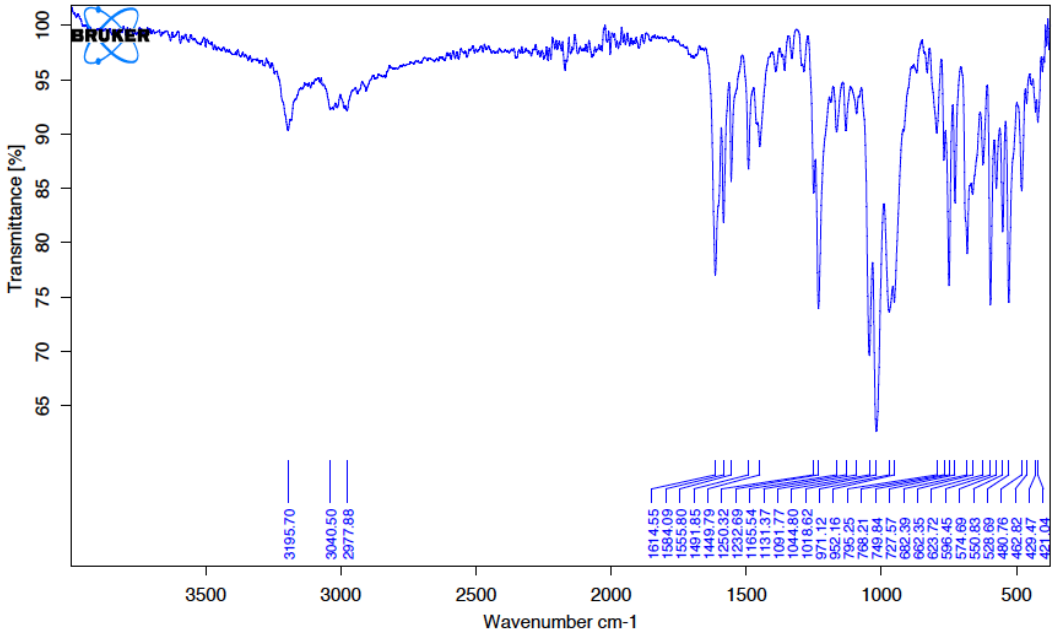

FT-IR spectrum

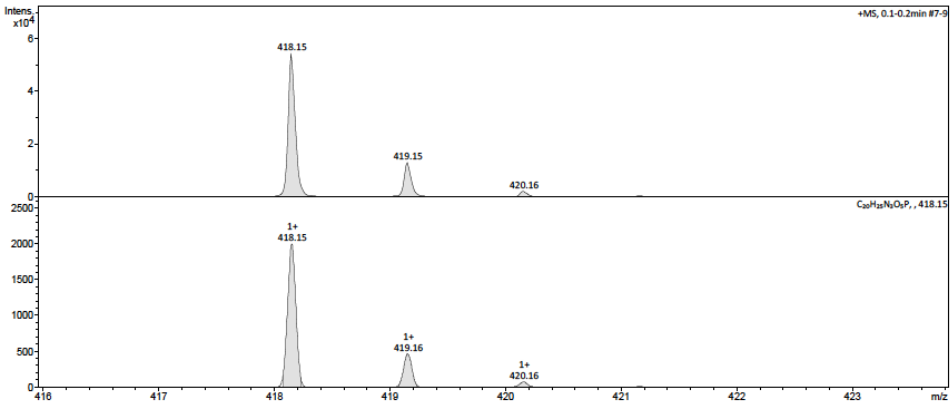

Mass spectrum (ESI-TOF)
exp. spectrum (top); calc. spectrum (bottom) for $C_{20}H_{24}O_5N_3P$ + H

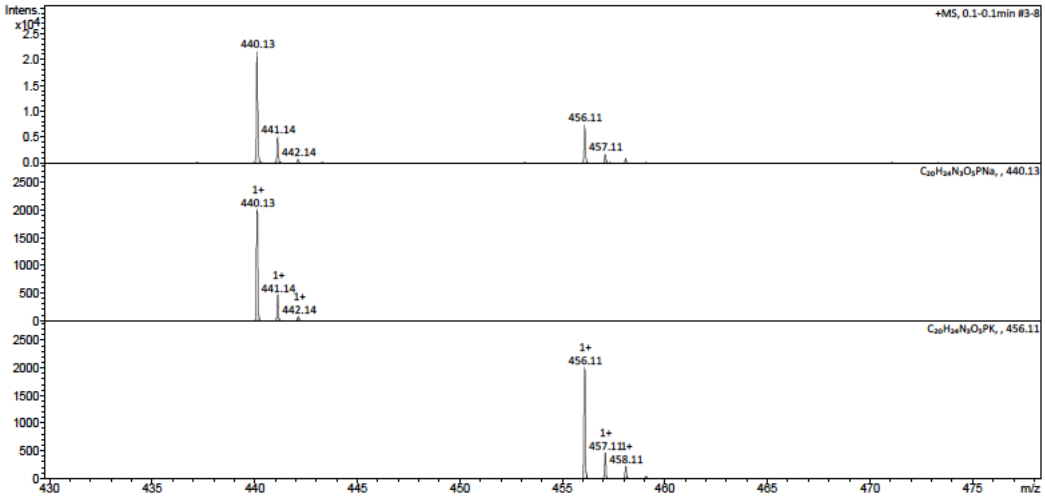

Mass spectrum (ESI-TOF)
exp. spectrum (top); calc. spectrum (middle) for $C_{20}H_{24}O_5N_3P$ + Na;
calc. spectrum (bottom) for $C_{20}H_{24}O_5N_3P$ + K

Diethyl[(5-phenyl-1,3,4-axodiazol-2-ylamino)(4-nitrophenyl)methyl]phosphonate (3c)

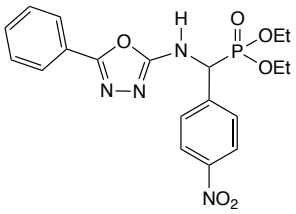

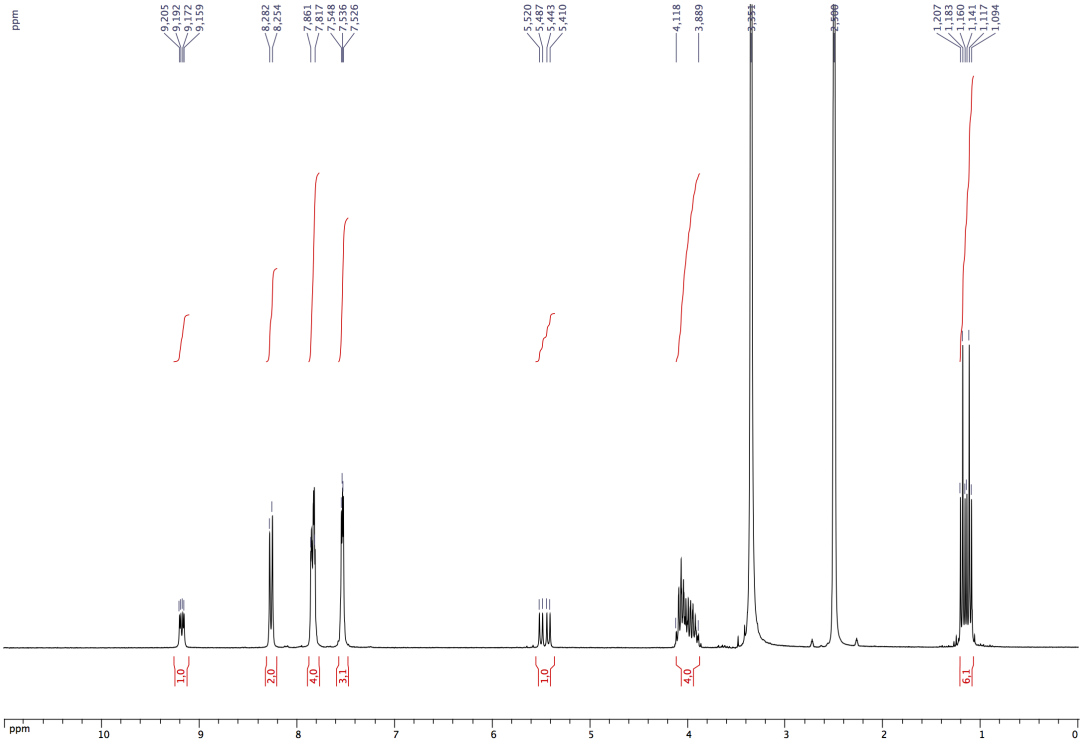

^{1}H NMR spectrum (DMSO-d_6)

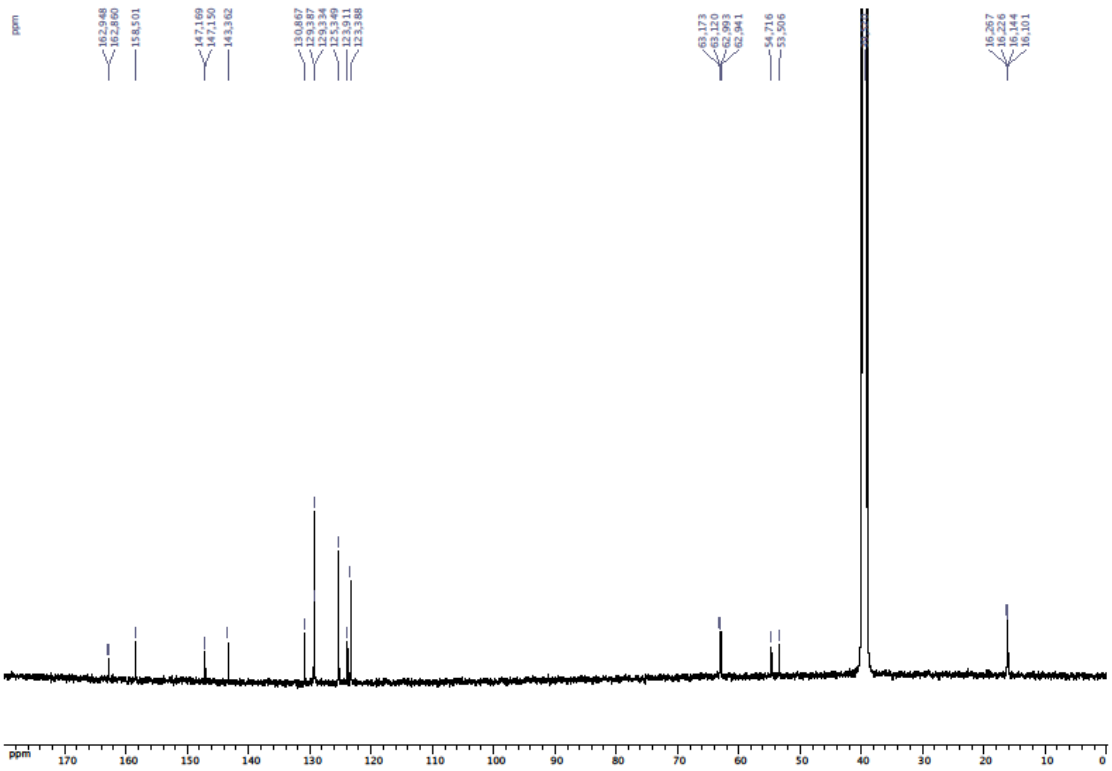

$^{13}C\{^{1}H\}$ NMR spectrum (DMSO-d_6)

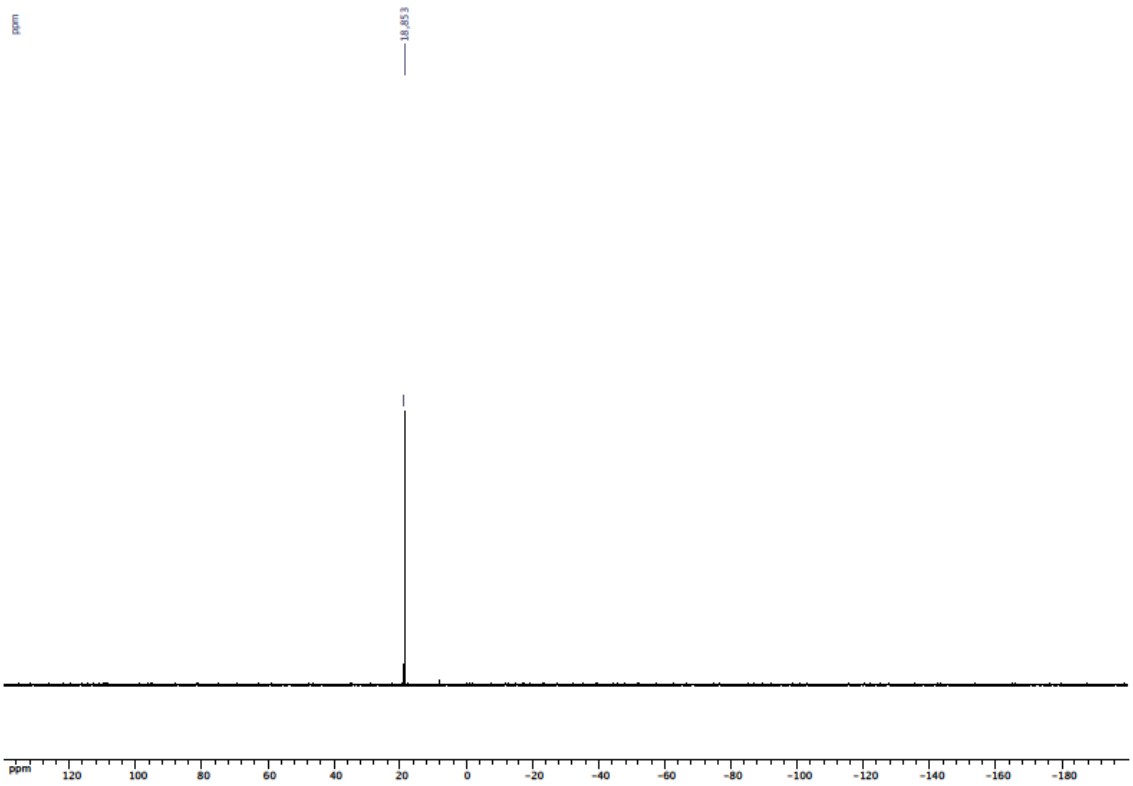

$^{31}P\{^{1}H\}$ NMR spectrum (DMSO-d_6)

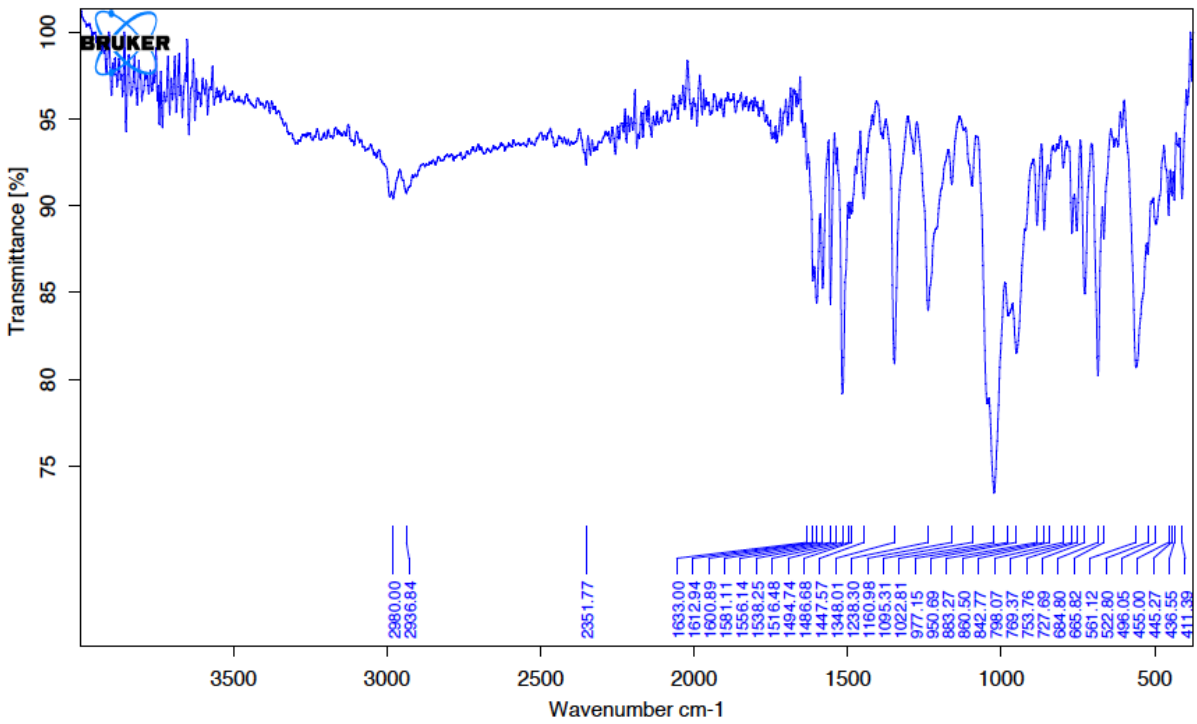

FT-IR spectrum

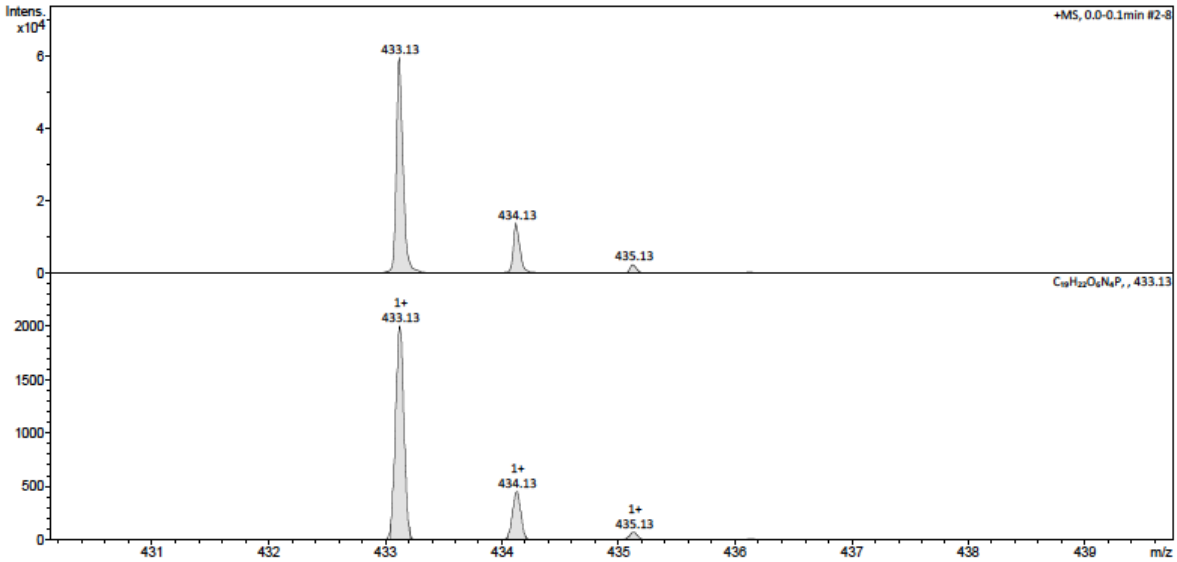

Mass spectrum (ESI-TOF)
exp. spectrum (top); calc. spectrum (bottom) for $C_{19}H_{21}O_6N_4P$ + H

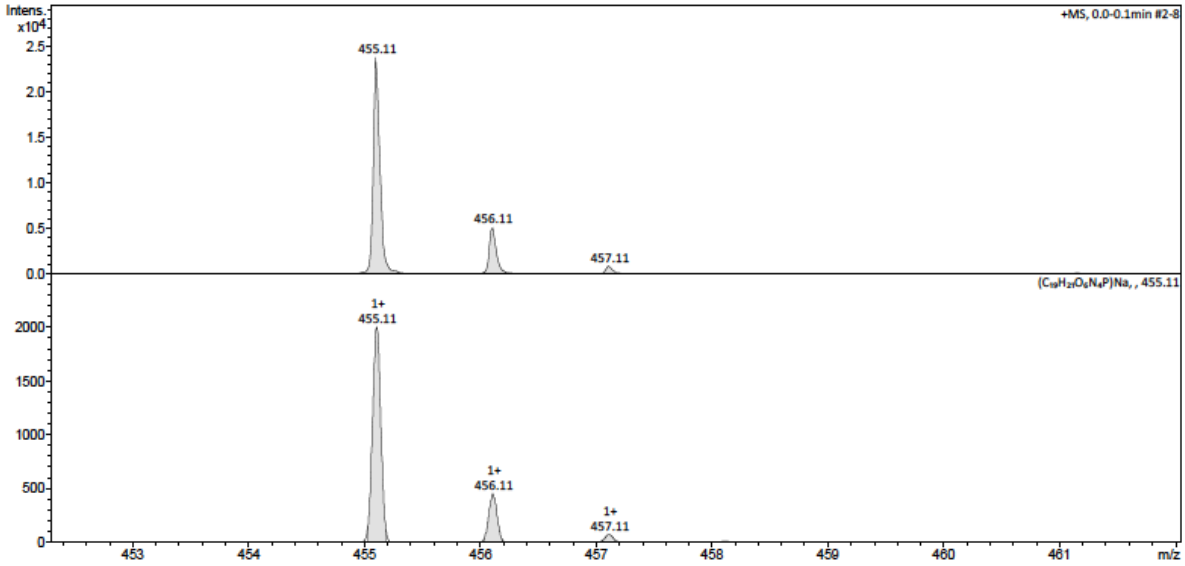

Mass spectrum (ESI-TOF)
exp. spectrum (top); calc. spectrum (bottom) for $C_{19}H_{21}O_6N_4P$ + Na

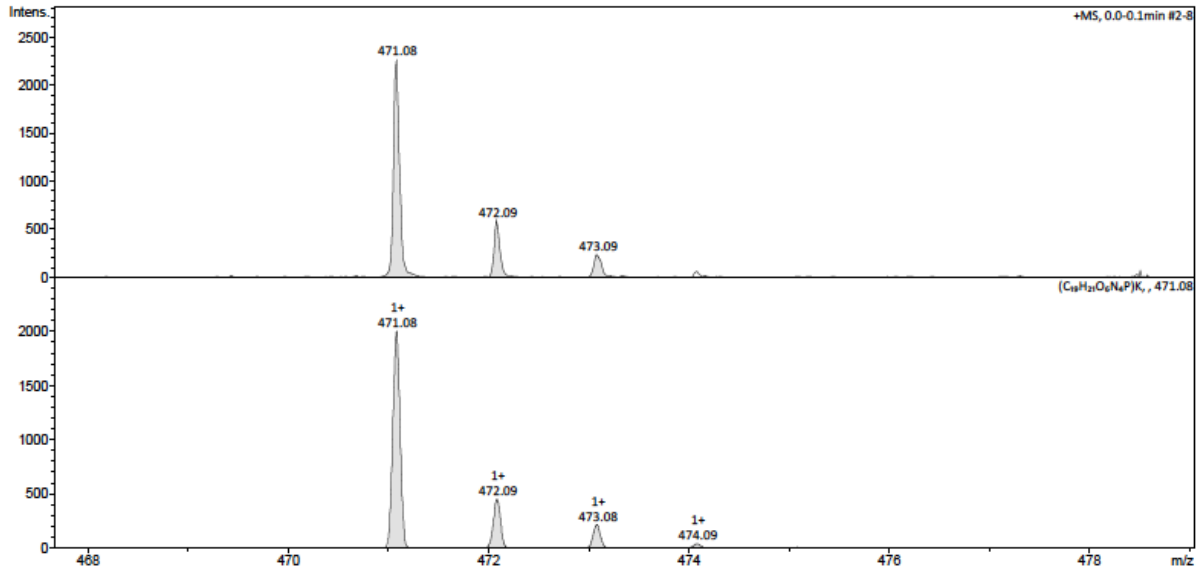

Mass spectrum (ESI-TOF)
exp. spectrum (top); calc. spectrum (bottom) for $C_{19}H_{21}O_6N_4P$ + K

Dichloro-{diethyl[(5-phenyl-1,3,4-axodiazol-2-ylamino)(4-trifluoromethylphenyl)methyl] phosphonate}(*p*-cymene) ruthenium(II) (4a)

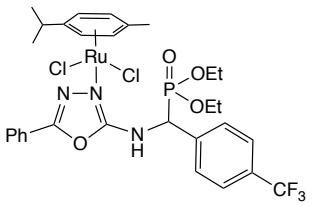

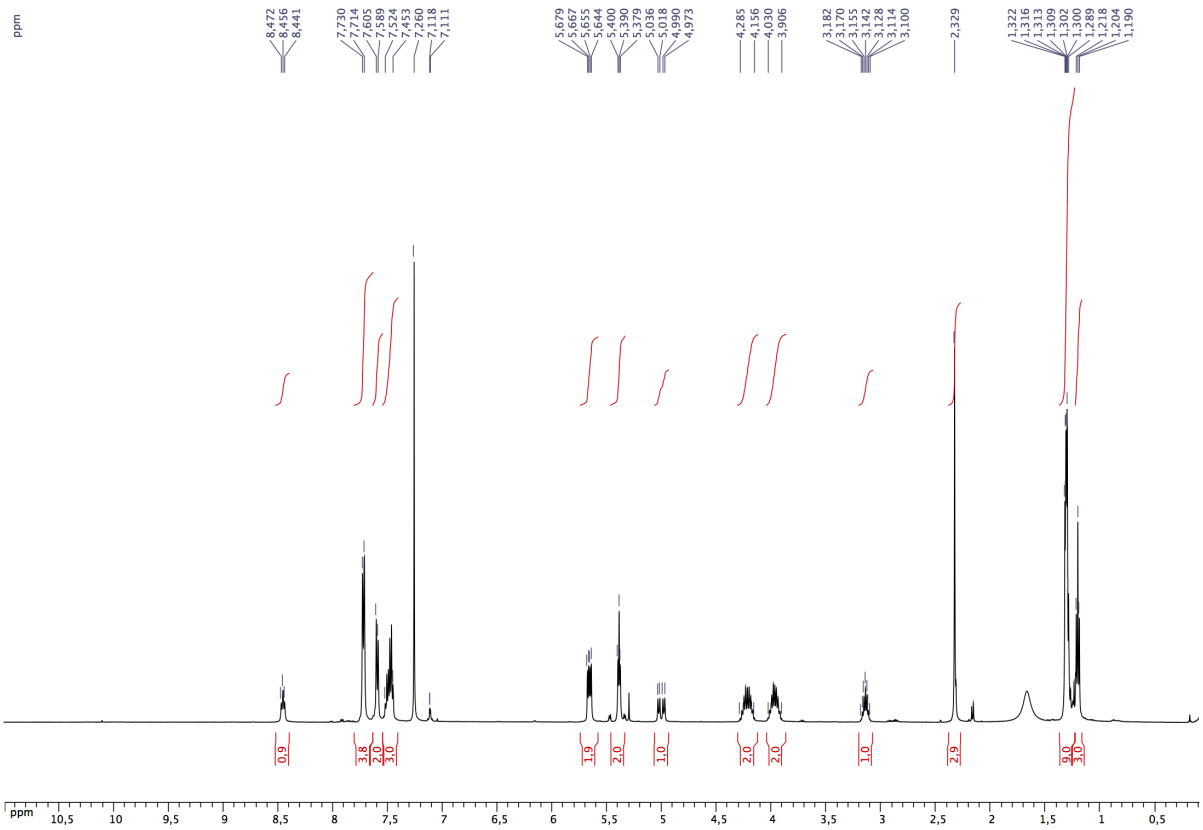

^{1}H NMR spectrum ($CDCl_3$)

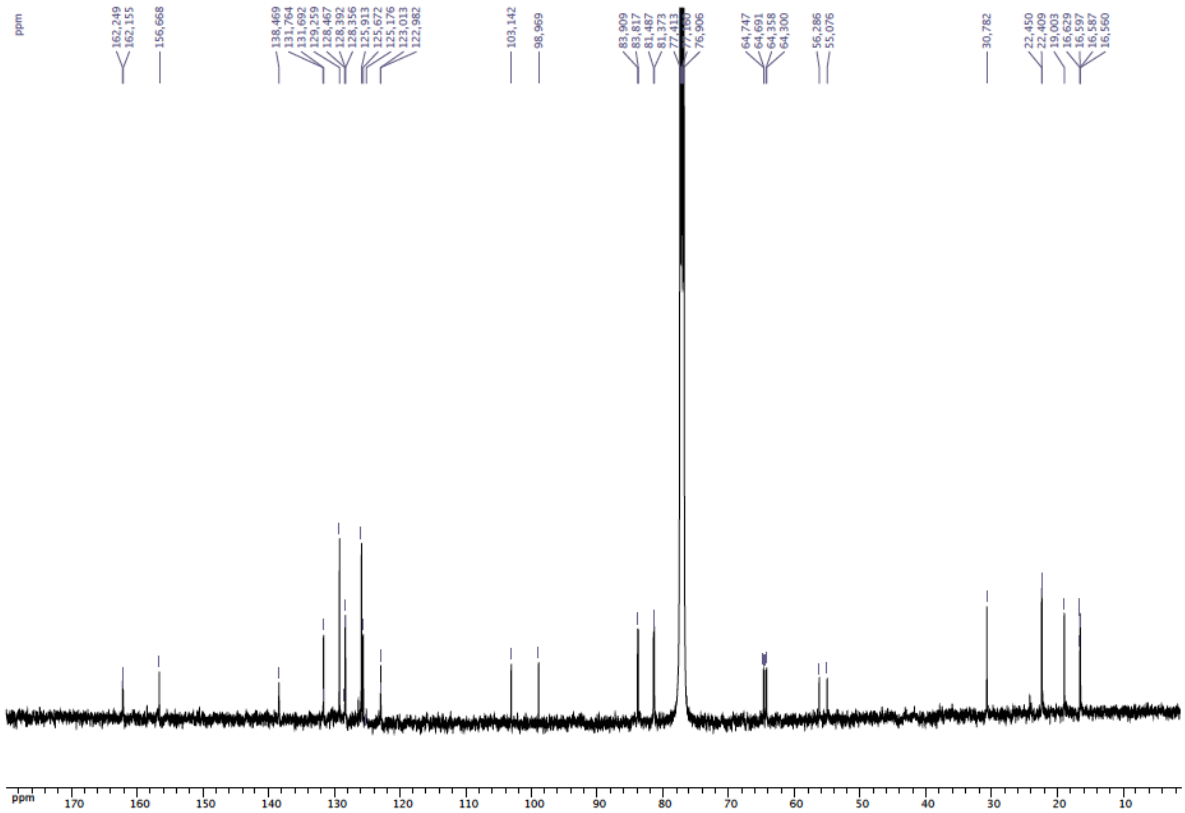

$^{13}C\{^{1}H\}$ NMR spectrum ($CDCl_3$)

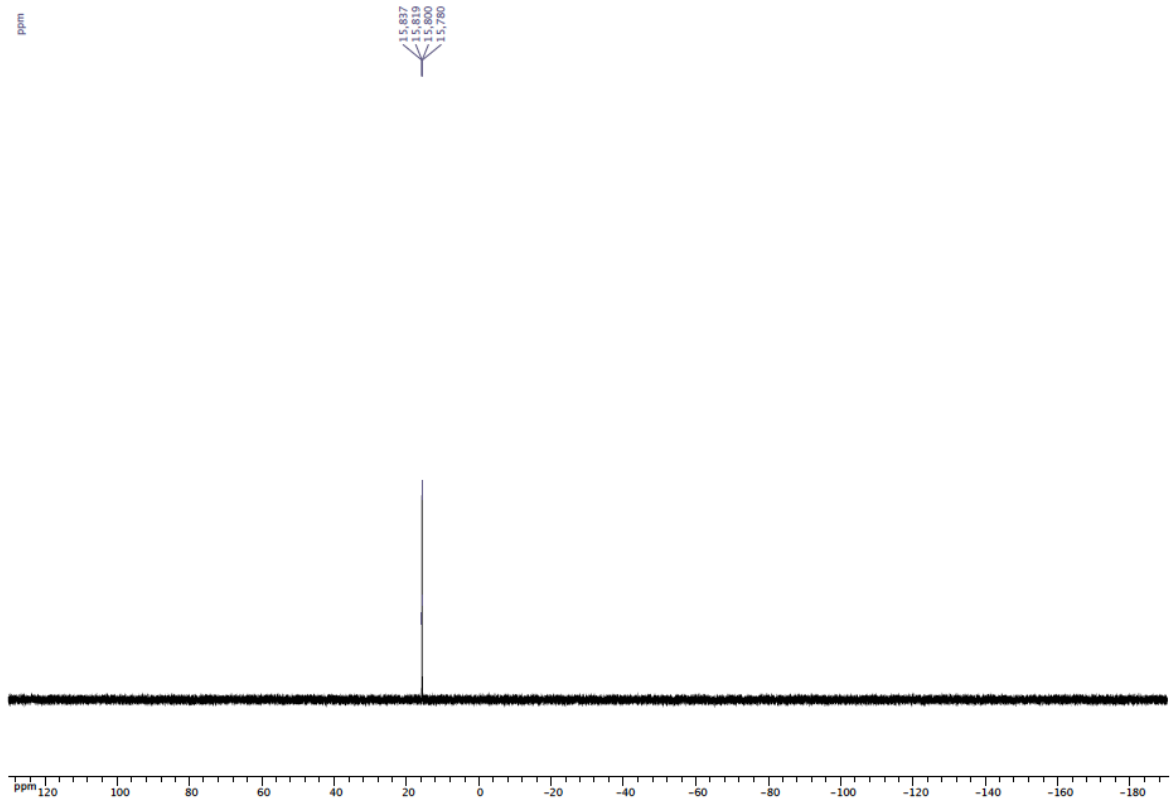

$^{31}P\{^{1}H\}$ NMR spectrum ($CDCl_3$)

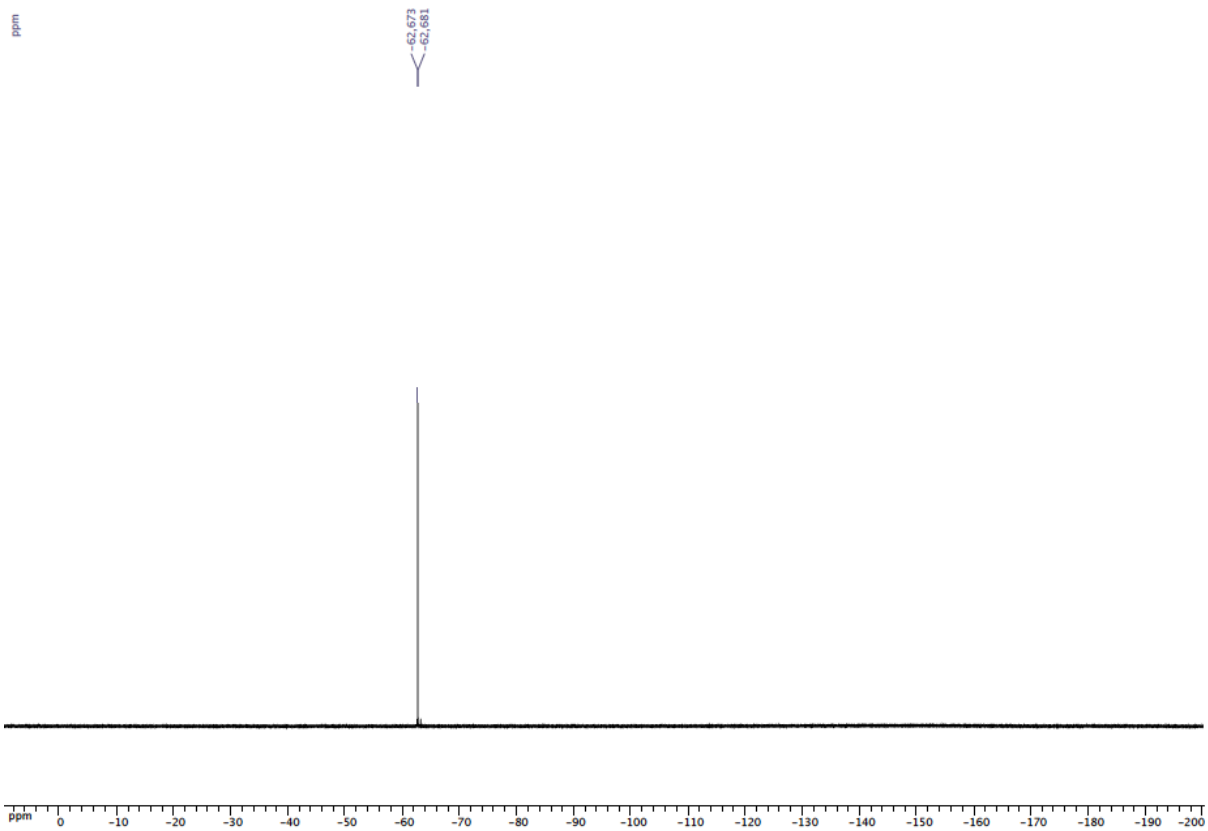

$^{19}F\{^{1}H\}$ NMR spectrum ($CDCl_3$)

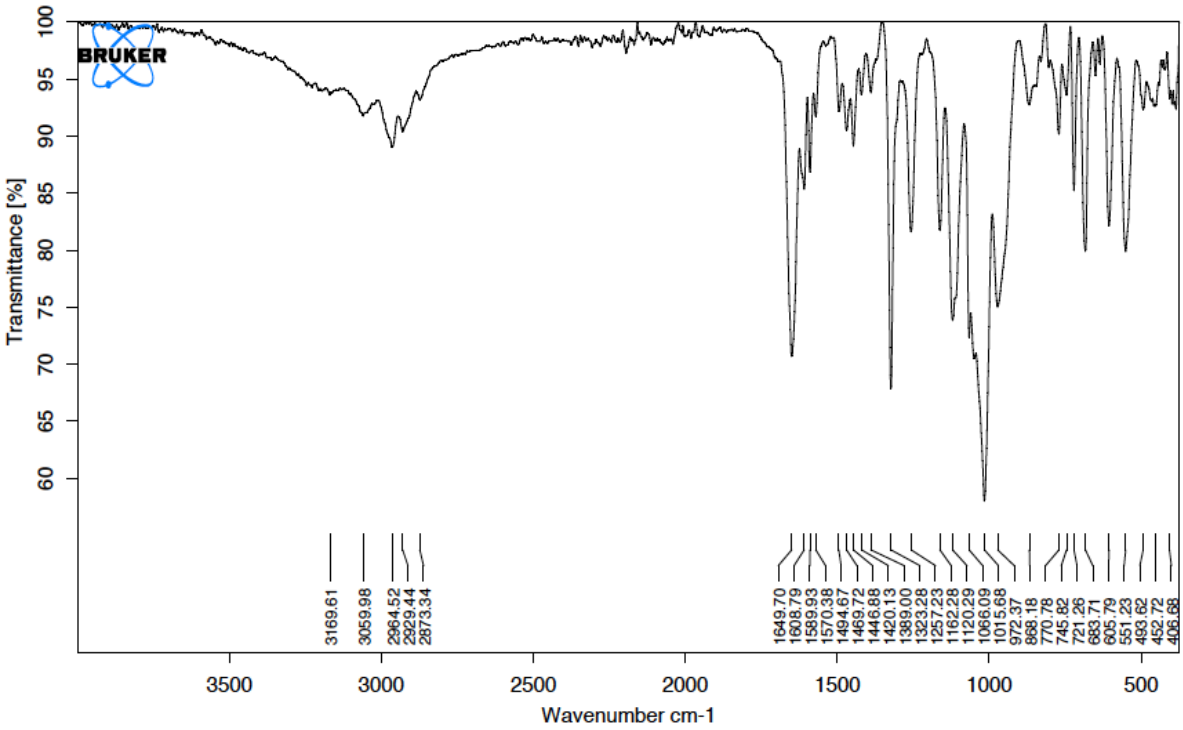

FT-IR spectrum

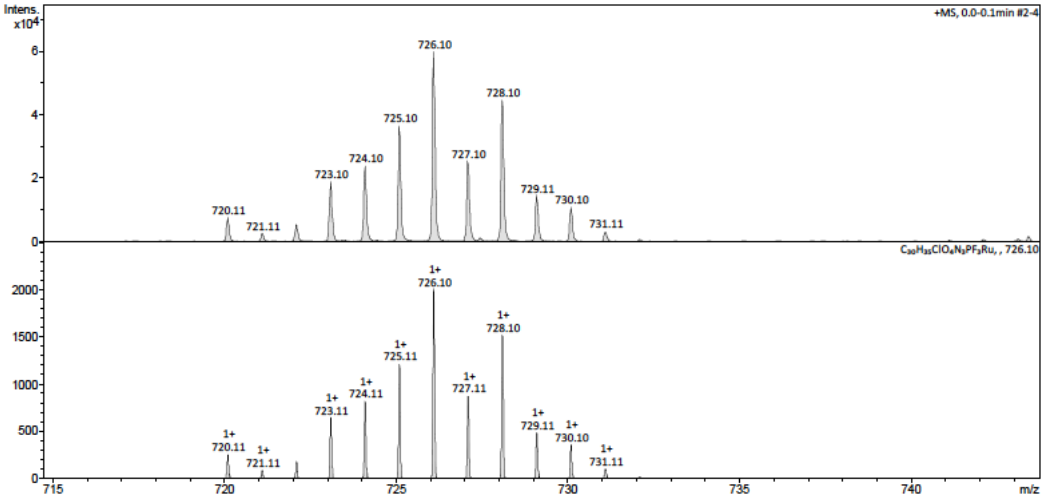

Mass spectrum (ESI-TOF)
exp. spectrum (top); calc. spectrum (bottom) for $C_{30}H_{35}O_4N_3PF_3ClRu$

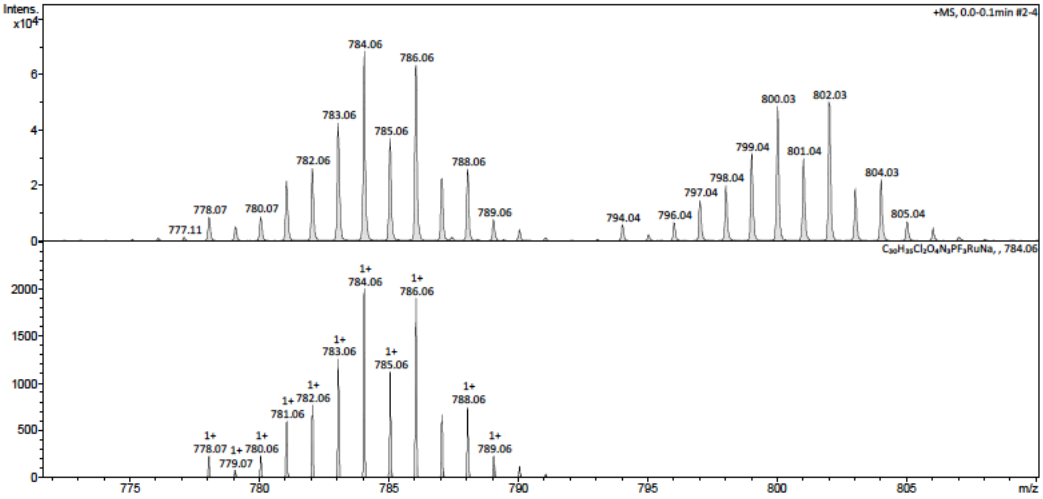

Mass spectrum (ESI-TOF)
exp. spectrum (top); calc. spectrum (bottom) for $C_{30}H_{35}O_4N_3PF_3Cl_2Ru + Na$

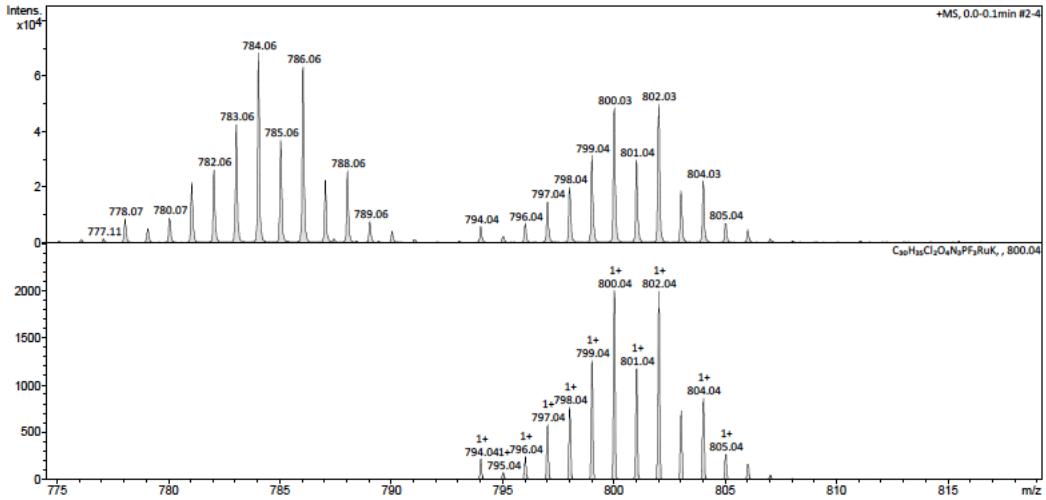

Mass spectrum (ESI-TOF)
exp. spectrum (top); calc. spectrum (bottom) for $C_{30}H_{35}O_4N_3PF_3Cl_2Ru + K$

Dichloro-{diethyl[(5-phenyl-1,3,4-axodiazol-2-ylamino)(2-methoxyphenyl)methyl] phosphonate}(*p*-cymene) ruthenium(II) (4b)

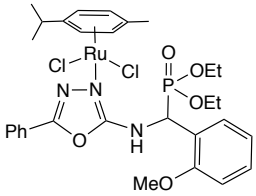

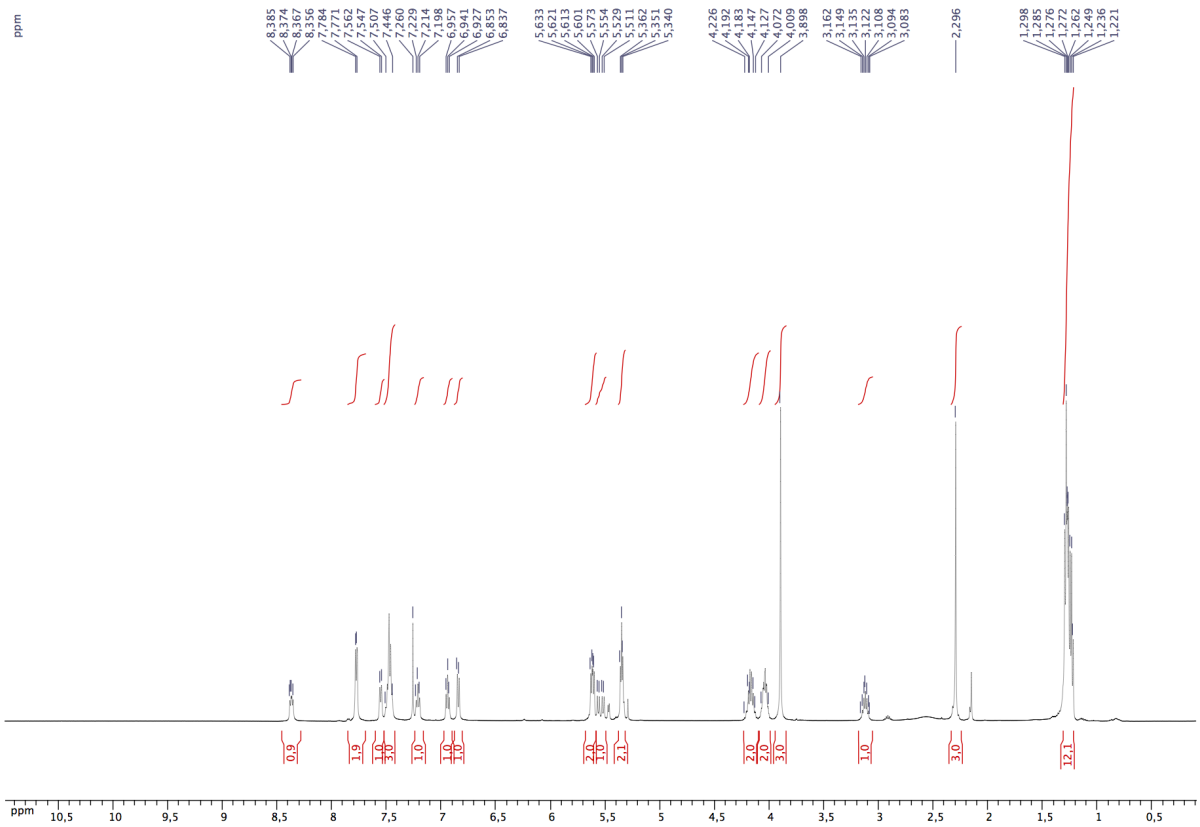

^{1}H NMR spectrum ($CDCl_3$)

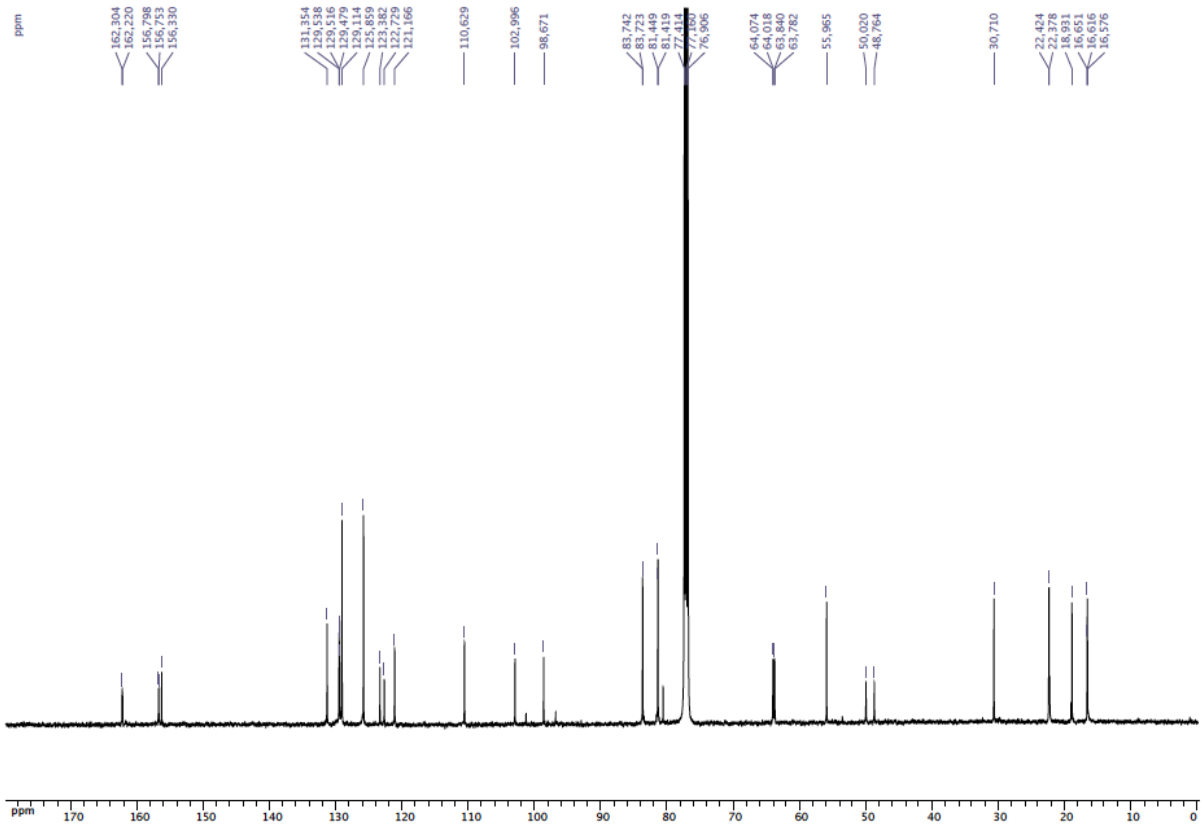

$^{13}C\{^{1}H\}$ NMR spectrum ($CDCl_3$)

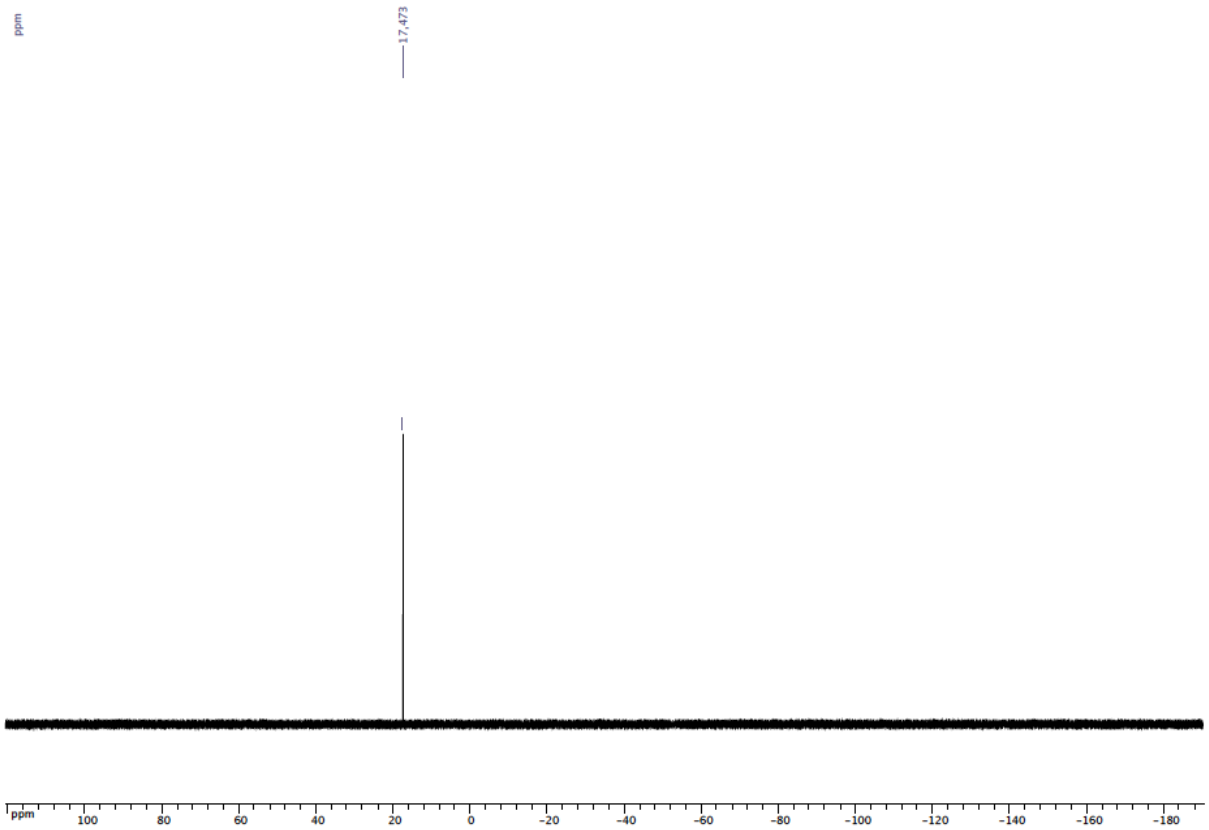

$^{31}P\{^{1}H\}$ NMR spectrum ($CDCl_3$)

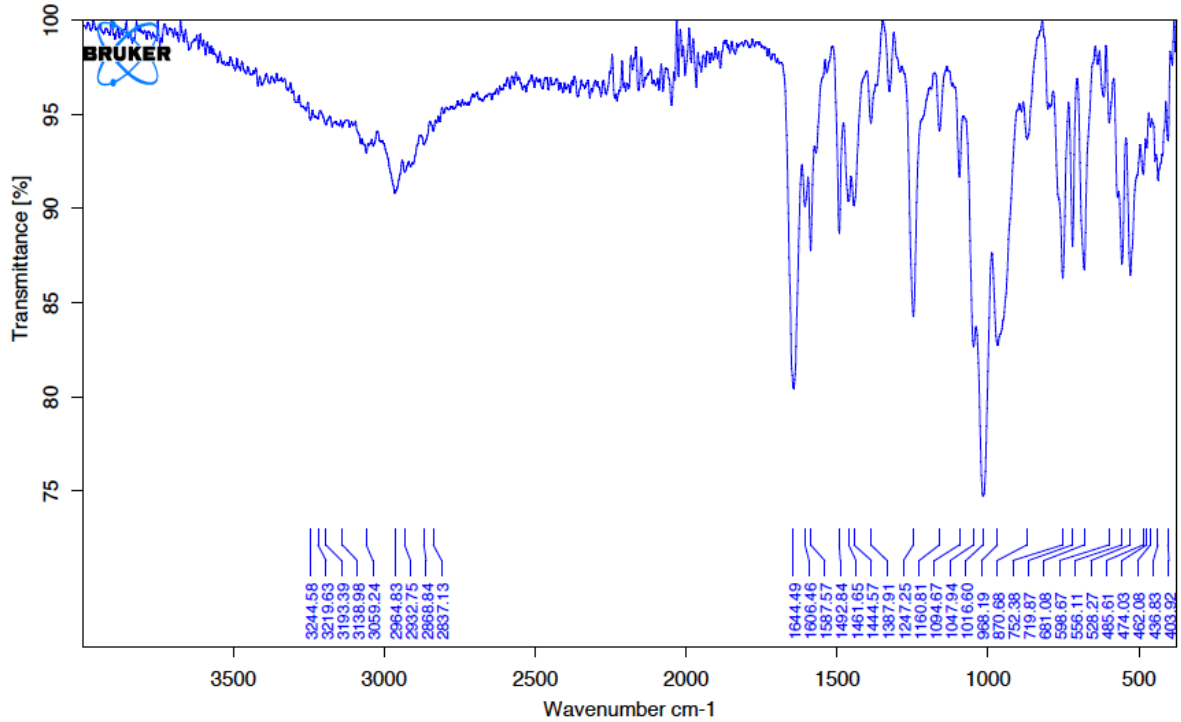

FT-IR spectrum

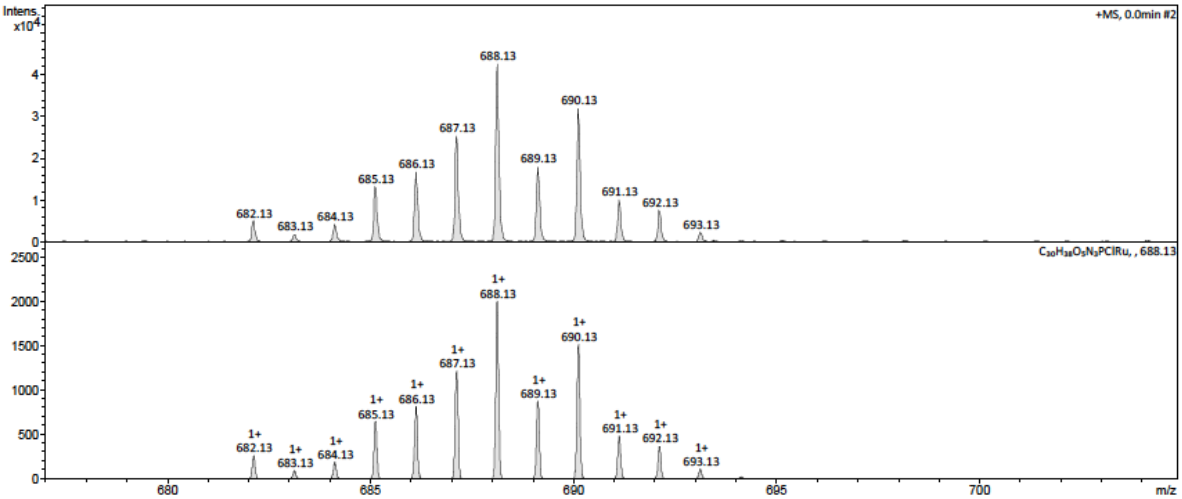

Mass spectrum (ESI-TOF)
exp. spectrum (top); calc. spectrum (bottom) for $C_{30}H_{38}O_5N_3PClRu$

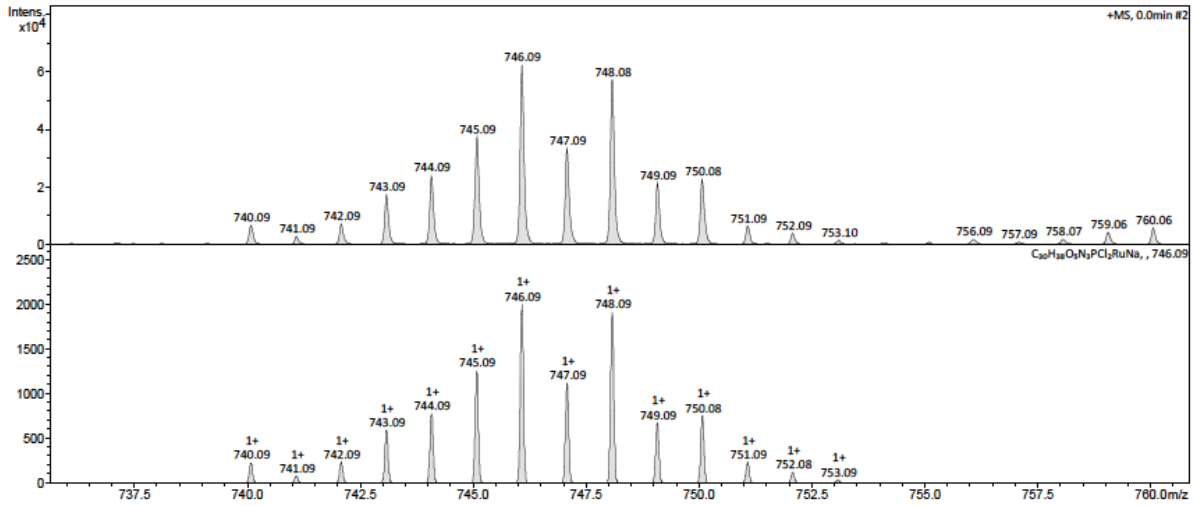

Mass spectrum (ESI-TOF)
exp. spectrum (top); calc. spectrum (bottom) for $C_{30}H_{38}O_5N_3PCl_2Ru$ + Na

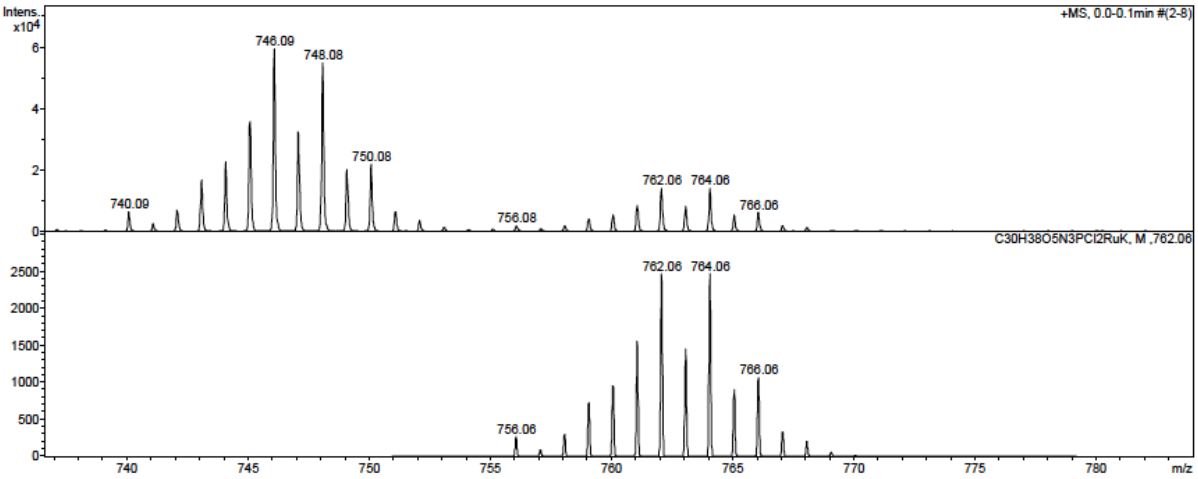

Mass spectrum (ESI-TOF)
exp. spectrum (top); calc. spectrum (bottom) for $C_{30}H_{38}O_5N_3PCl_2Ru$ + K

Dichloro-{diethyl[(5-phenyl-1,3,4-axodiazol-2-ylamino)(4-nitrophenyl)methyl] phosphonate}(*p*-cymene) ruthenium(II) (4c)

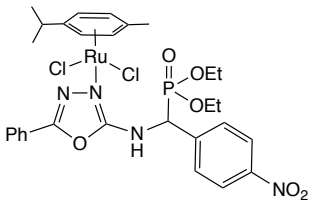

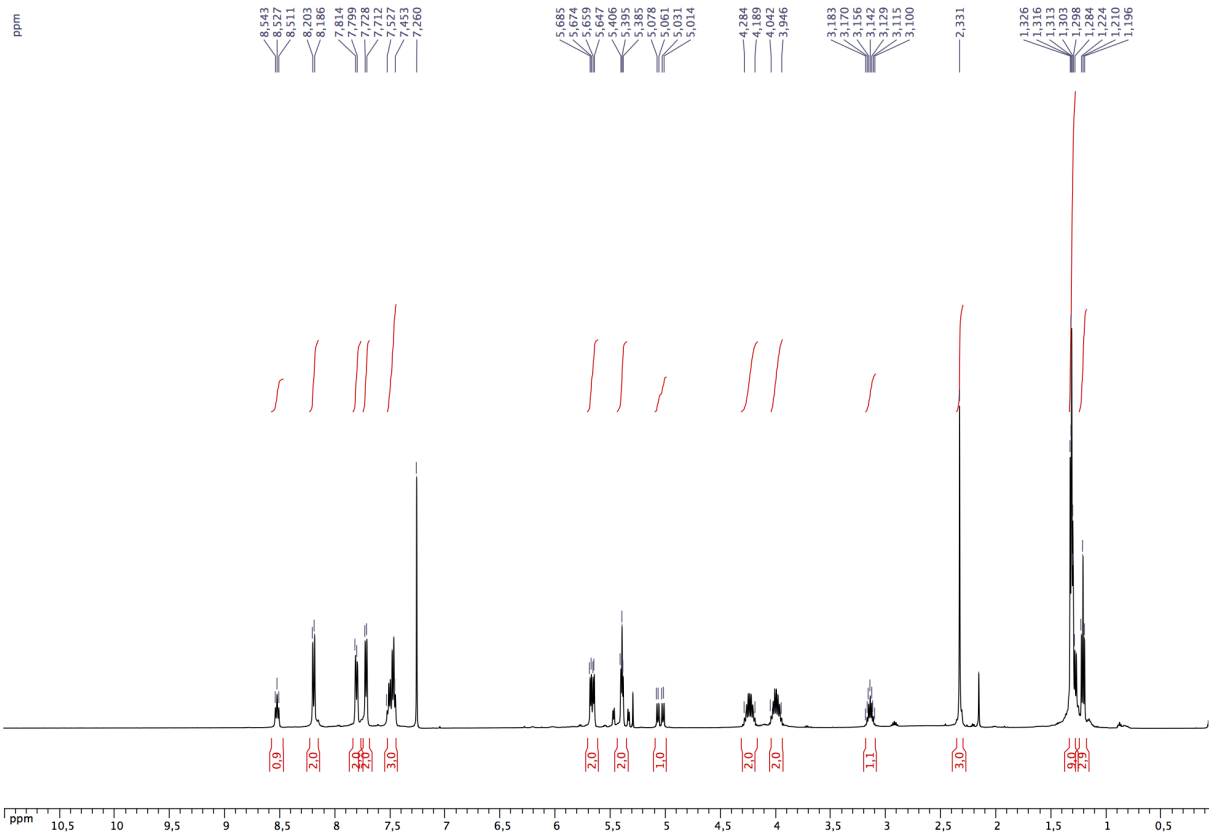

^{1}H NMR spectrum ($CDCl_3$)

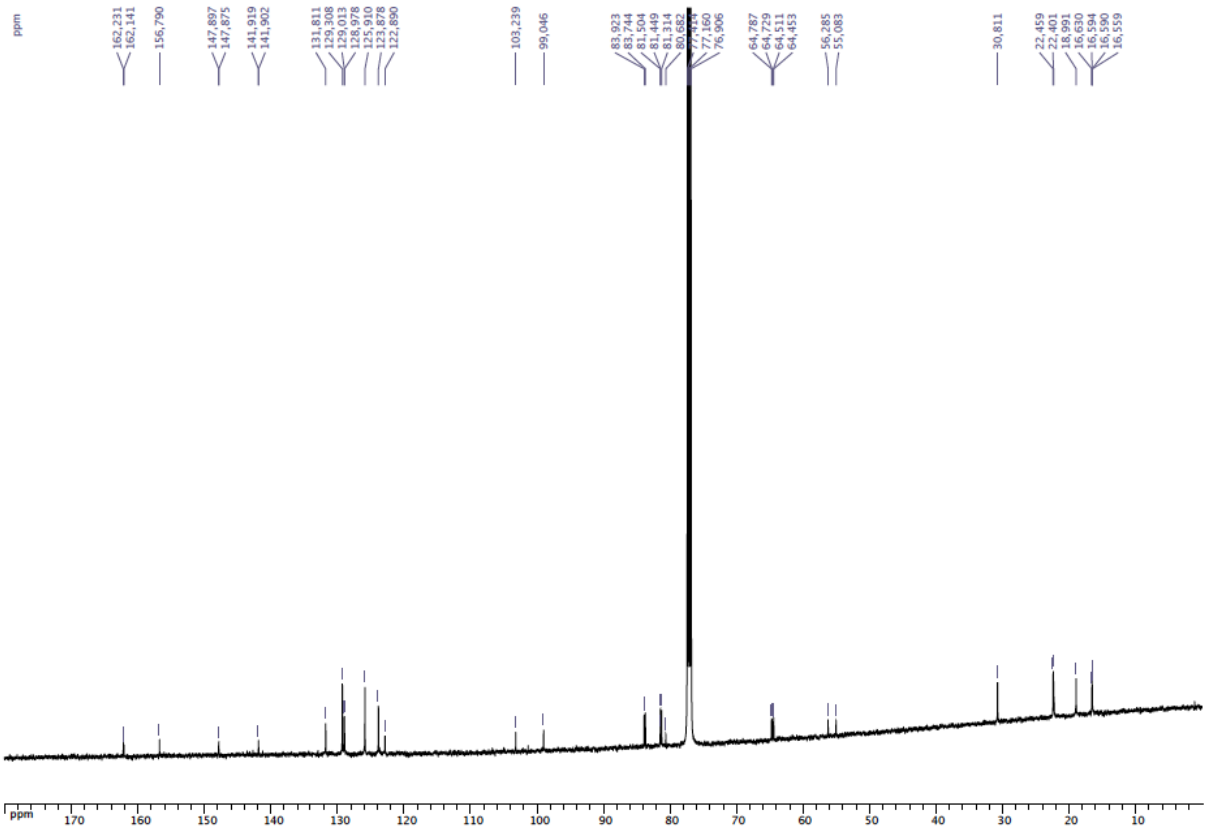

$^{13}C\{^{1}H\}$ NMR spectrum ($CDCl_3$)

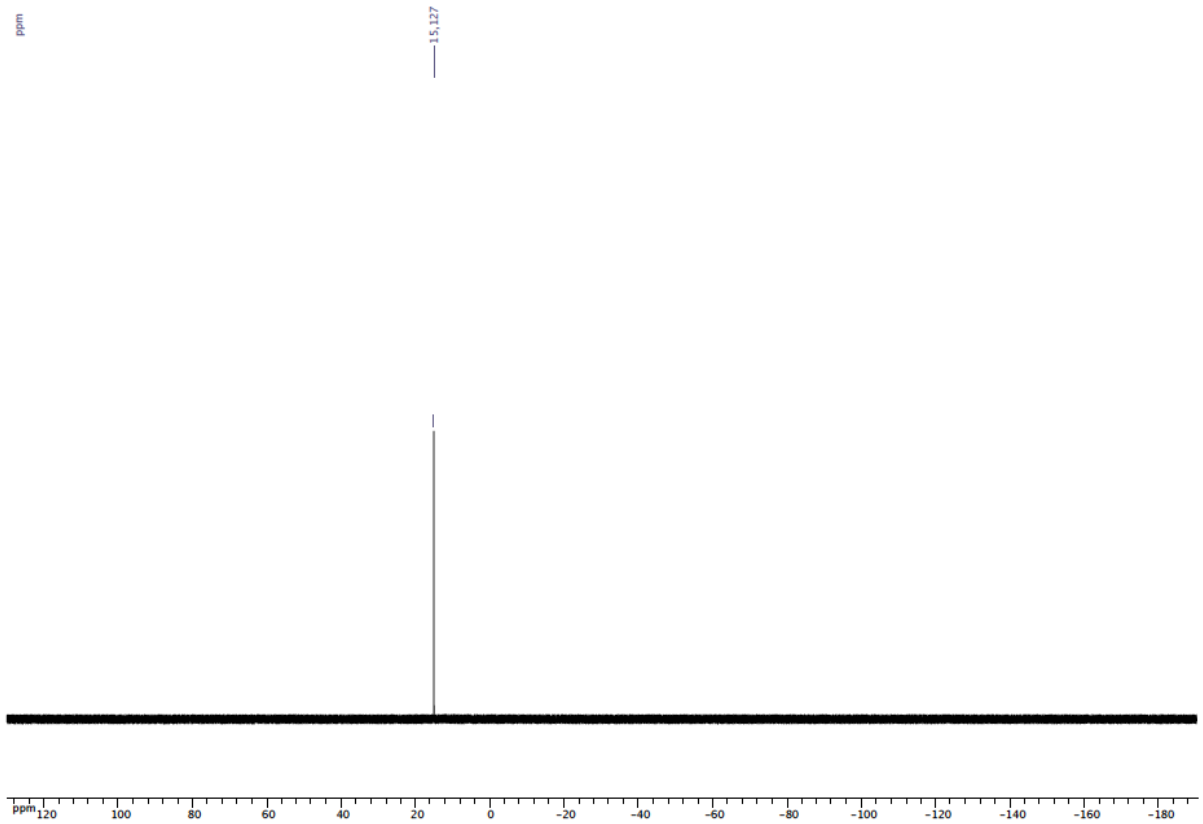

$^{31}P\{^{1}H\}$ NMR spectrum ($CDCl_3$)

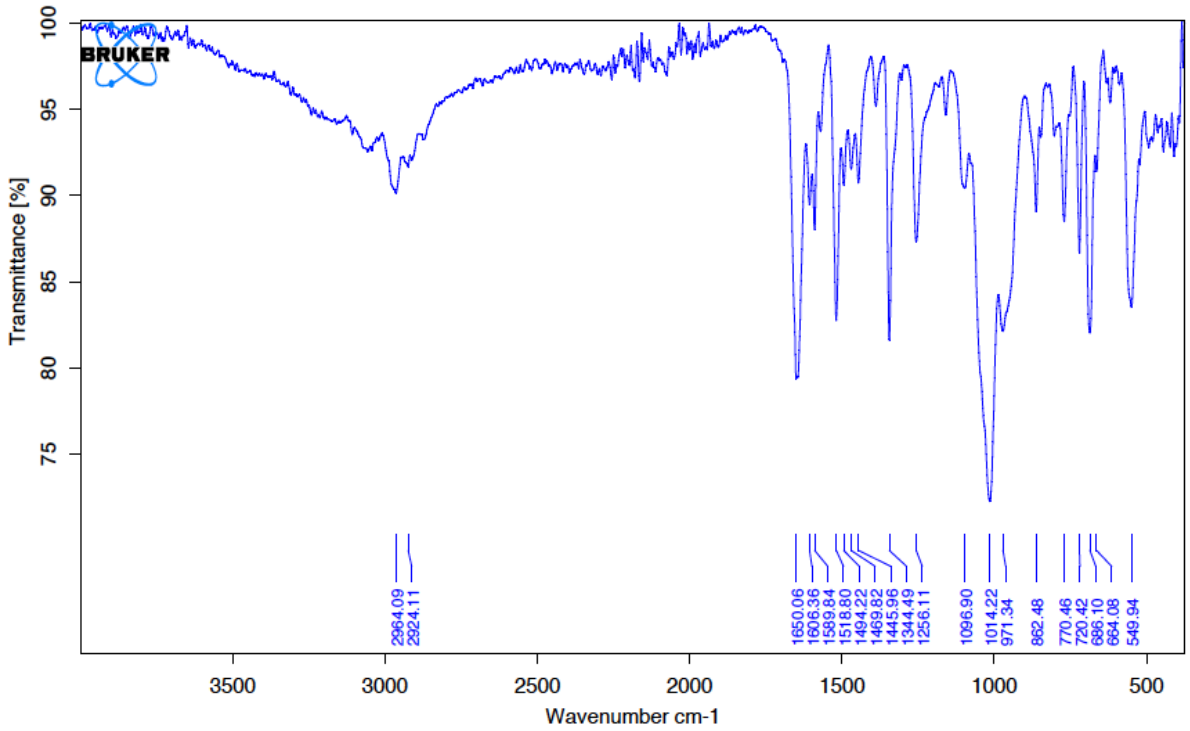

FT-IR spectrum

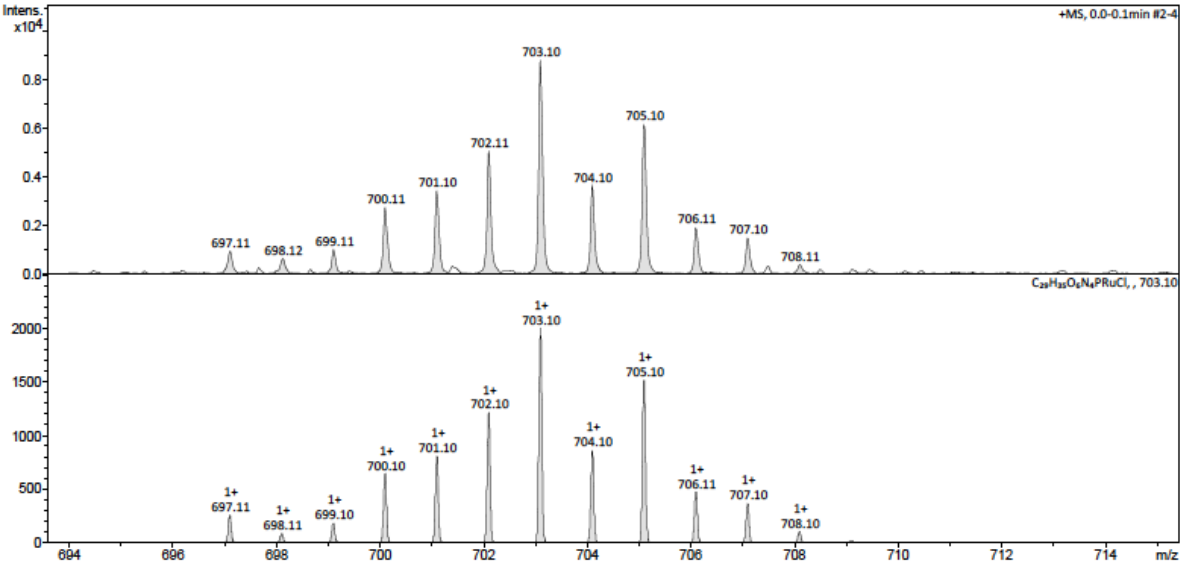

Mass spectrum (ESI-TOF)
exp. spectrum (top); calc. spectrum (bottom) for $C_{29}H_{35}O_6N_4PClRu$

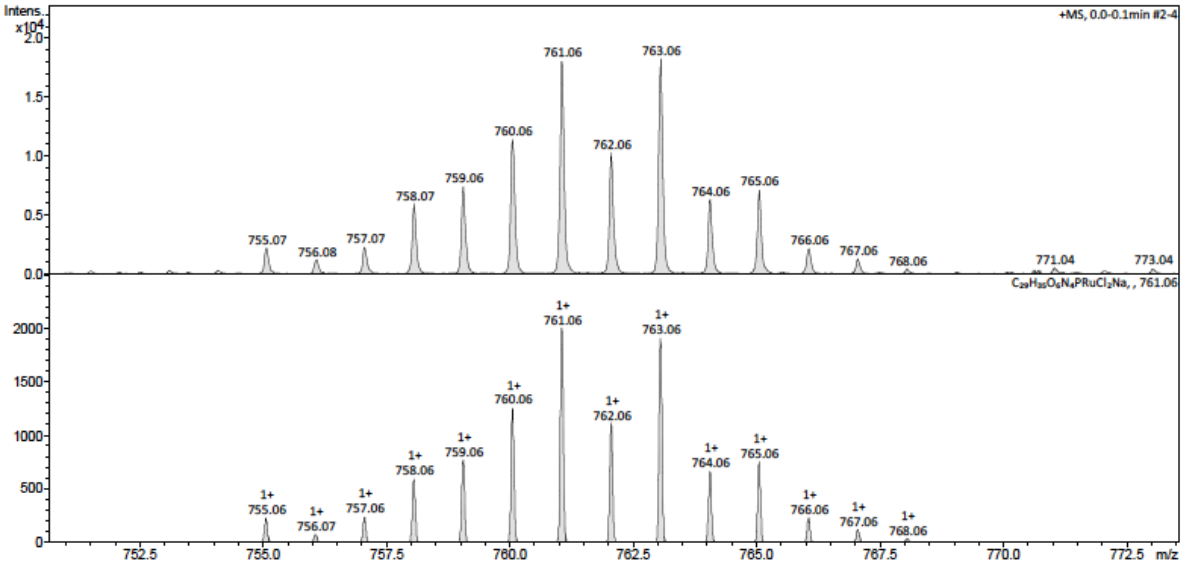

Mass spectrum (ESI-TOF)
exp. spectrum (top); calc. spectrum (bottom) for $C_{29}H_{35}O_6N_4PCl_2Ru$ + Na

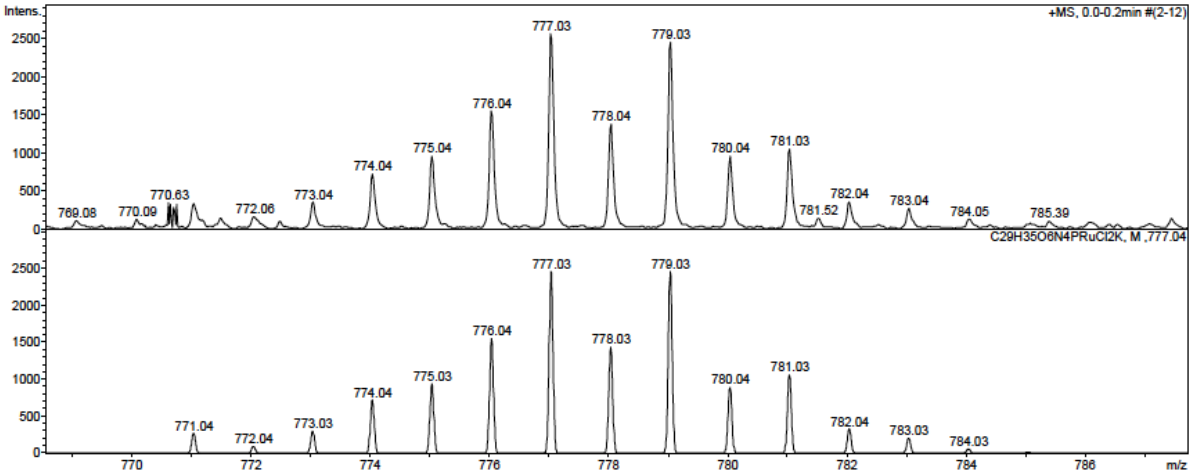

Mass spectrum (ESI-TOF)
exp. spectrum (top); calc. spectrum (bottom) for $C_{29}H_{35}O_6N_4PCl_2Ru$ + K

NMR description of the catalytic products

1-Phenylethan-1-ol: ^{1}H NMR (500 MHz, $CDCl_3$): δ = 7.33 (d, 2H, arom. CH, $^3J_{HH}$ = 7.5 Hz), 7.28 (dd, 2H, arom. CH, $^3J_{HH}$ = 7.5 Hz, $^4J_{HH}$ = 2.0 Hz), 7.20 (t, 1H, arom. CH, $^3J_{HH}$ = 4.5 Hz), 4.84 (q, 1H, CH(OH), $^3J_{HH}$ = 6.5 Hz), 1.44 (d, 3H, CH_3, $^3J_{HH}$ = 6.5 Hz) ppm; **^{13}C{^{1}H} NMR (126 MHz, $CDCl_3$):** δ = 146.02 (s, arom. Cquat of C_6H_5), 128.22 (s, arom. CH meta of Cquat), 127.07 (s, arom. CH para of Cquat), 125.29 (s, arom. CH ortho of Cquat), 69.95 (s, CH(OH)), 25.17 (s, CH_3) ppm.

1-(4-Bromophenyl)ethan-1-ol: ^{1}H NMR (500 MHz, $CDCl_3$): δ = 7.47 (d, 2H, arom. CH, $^3J_{HH}$ = 8.5 Hz), 7.25 (d, 2H, arom. CH, $^3J_{HH}$ = 8.5 Hz), 4.86 (q, 1H, CH(OH), $^3J_{HH}$ = 6.0 Hz), 1.47 (d, 3H, CH_3, $^3J_{HH}$ = 6.0 Hz) ppm; **^{13}C{^{1}H} NMR (126 MHz, $CDCl_3$):** δ = 144.86 (s, arom. Cquat of C_6H_4Br), 131.67 (s, arom. CH ortho of CBr), 127.27 (s, arom. CH meta of CBr), 121.28 (s, arom. Cquat CBr), 69.92 (s, CH(OH)), 25.40 (s, CH_3) ppm.

1-(2-Bromophenyl)ethan-1-ol: ^{1}H NMR (500 MHz, $CDCl_3$): δ = 7.56 (d, 1H, arom. CH, $^3J_{HH}$ = 7.5 Hz), 7.48 (d, 1H, arom. CH, $^3J_{HH}$ = 8.0 Hz), 7.31 (t, 1H, arom, $^3J_{HH}$ = 7.7 Hz), 7.09 (t, 1H, arom, $^3J_{HH}$ = 8.0 Hz), 5.19 (q, 1H, CH(OH), $^3J_{HH}$ = 6.5 Hz), 1.44 (d, 3H, CH_3, $^3J_{HH}$ = 6.5 Hz)ppm; **^{13}C{^{1}H} NMR (126 MHz, $CDCl_3$):** δ = 144.86 (s, arom. Cquat of C_6H_4Br), 132.63 (s, arom. CH ortho of CBr), 128.73 (s, arom. CH meta of CBr), 127.87 (s, arom. CH para of CBr), 126.77 (s, arom. CH meta of CBr), 121.69 (s, arom. Cquat CBr), 69.12 (s, CH(OH)), 23.71 (s, CH_3) ppm.

1-(4-Methoxyphenyl)ethan-1-ol: ^{1}H NMR (500 MHz, $CDCl_3$): δ = 7.27 (d, 2H, arom. CH, $^3J_{HH}$ = 8.5 Hz), 6.85 (d, 2H, arom. CH, $^3J_{HH}$ = 8.5 Hz), 4.82 (q, 1H, CH(OH), $^3J_{HH}$ = 6.5 Hz), 3.77 (s, 3H, OCH_3), 1.45 (d, 3H, CH_3, $^3J_{HH}$ = 6.5 Hz) ppm; **^{13}C{^{1}H} NMR (126 MHz, $CDCl_3$):** δ = 158.96 (s, arom. Cquat *C*OCH_3), 138.19 (s, arom. Cquat $C_6H_4OCH_3$), 126.71 (s, arom. CH meta of $COCH_3$), 113.85 (s, arom. CH ortho of $COCH_3$), 69.92 (s, CH(OH)), 55.33 (s, OCH_3), 23.99 (s, CH_3) ppm.

1-(4-Nitrophenyl)ethan-1-ol: ^{1}H NMR (500 MHz, $CDCl_3$): δ = 8.19 (d, 1H, arom. CH, $^3J_{HH}$ = 8.5 Hz), 7.54 (d, 1H, arom. CH, $^3J_{HH}$ = 8.5 Hz), 5.02 (q, 1H, CH(OH), $^3J_{HH}$ = 6.5 Hz), 1.51 (d, 3H, CH_3, $^3J_{HH}$ = 6.5 Hz) ppm; **^{13}C{^{1}H} NMR (126 MHz, $CDCl_3$):** δ = 153.22 (s, arom. Cquat CNO_2), 150.95 (s, arom. Cquat of $C_6H_4NO_2$), 131.32 (s, arom. CH meta of CNO_2), 126.25 (s, arom. CH ortho of CNO_2), 68.08 (s, CH(OH)), 25.72 (s, CH_3) ppm.

1-(4-Chlorophenyl)ethan-1-ol: ^{1}H NMR (500 MHz, $CDCl_3$): δ = 7.28-7.22 (m, 4H, arom. CH), 4.84 (q, 1H, CH(OH), $^3J_{HH}$ = 8.5 Hz), 1.44 (d, 3H, CH_3, $^3J_{HH}$ = 8.5 Hz) ppm; **^{13}C{^{1}H} NMR (126 MHz, $CDCl_3$):** δ = 144.56 (s, arom. Cquat of C_6H_4Cl), 139.33 (s, arom. CH

ortho of CCl), 135.16 (s, arom. CH meta of CCl), 132.50 (s, arom. Cquat CCl), 69.20 (s, CH(OH)), 25.16 (s, CH_3) ppm.

1-(2,4-Dichlorophenyl)ethan-1-ol: ^{1}H NMR (500 MHz, $CDCl_3$): δ = 7.48 (d, 1H, arom. CH, $^3J_{HH}$ = 8.5 Hz), 7.26 (dd, 1H, arom. CH, $^3J_{HH}$ = 8.5 Hz, $^4J_{HH}$ = 1.5 Hz), 7.24 (d, 1H, arom. CH, $^4J_{HH}$ = 1.5 Hz), 5.17 (q, 1H, CH(OH), $^3J_{HH}$ = 6.0 Hz), 1.39 (d, 3H, CH_3, $^3J_{HH}$ = 6.0 Hz) ppm; **^{13}C{^{1}H} NMR (126 MHz, $CDCl_3$):** δ = 141.92 (s, arom. Cquat of $C_6H_3Cl_2$), 137.27 (s, arom. Cquat CCl para of CCH(OH)), 132.25 (s, arom. Cquat CCl ortho of CCH(OH)), 129.18 (s, arom. CH CCl*C*HCCl), 127.60 (s, arom. CH ortho of CCH(OH)), 127.59 (s, arom. CH meta of CCH(OH)), 66.67 (s, CH(OH)), 23.74 (s, CH_3) ppm.

Cyclopentanol: ^{1}H NMR (500 MHz, $CDCl_3$): δ = 4.33-4.27 (m, 1H, CH(OH)), 1.93-1.76 (m, 8H, CH_2) ppm; **^{13}C{^{1}H} NMR (126 MHz, $CDCl_3$):** δ = 73.98 (s, CH(OH)), 35.57 (s, CH_2 ortho of CH(OH)), 23.33 (s, CH_2 meta of CH(OH)) ppm.

Cyclohexanol: ^{1}H NMR (500 MHz, $CDCl_3$): δ = 3.54-3.51 (m, 1H, CH(OH)), 1.85-1.79 (m, 2H, CH_2), 1.69-1.64 (m, 2H, CH_2), 1.50-1.45 (m, 1H, CH_2), 1.25-1.08 (m, 5H, CH_2) ppm; **^{13}C{^{1}H} NMR (126 MHz, $CDCl_3$):** δ = 70.20 (s, CH(OH)), 35.49 (s, CH_2 ortho of CH(OH)), 25.50 (s, CH_2 para of CH(OH)), 24.21 (s, CH_2 meta of CH(OH)) ppm.

3,3-Dimethylbutan-2-ol: ^{1}H NMR (500 MHz, $CDCl_3$): δ = 3.46 (q, 1H, CH(OH), $^3J_{HH}$ = 6.5 Hz), 1.48 (d, 3H, CH_3, $^3J_{HH}$ = 6.5 Hz), 0.89 (s, 9H, CH_3) ppm; **^{13}C{^{1}H} NMR (126 MHz, $CDCl_3$):** δ = 75.82 (s, CH(OH)), 35.04 (s, Cquat), 25.82 (s, C(CH$_3$)$_3$), 18.02 (s, CH(OH)CH$_3$) ppm.